Atmos. Chem. Phys. Discuss., 14, 11103–11152, 2014
www.atmos-chem-phys-discuss.net/14/11103/2014/
doi:10.5194/acpd-14-11103-2014

Atmospheric Chemistry and Physics Discussions
Open Access

Air quality simulations of wildfires in the Pacific Northwest evaluated with surface and satellite observations during the summers of 2007 and 2008

F. L. Herron-Thorpe[1], G. H. Mount[1], L. K. Emmons[2], B. K. Lamb[1], D. A. Jaffe[3,4], N. L. Wigder[3,4], S. H. Chung[1], R. Zhang[1], M. D. Woelfle[3], and J. K. Vaughan[1]

[1]Laboratory for Atmospheric Research, Washington State University, Pullman, WA, USA
[2]National Center for Atmospheric Research, Boulder, CO, USA
[3]Department of Atmospheric Sciences, University of Washington, Seattle, WA, USA
[4]Science and Technology Program, University of Washington-Bothell, Bothell, WA, USA

Received: 26 February 2014 – Accepted: 7 April 2014 – Published: 6 May 2014

Correspondence to: F. L. Herron-Thorpe (farrenthorpe@wsu.edu)

Published by Copernicus Publications on behalf of the European Geosciences Union.

Abstract

Evaluation of a regional air quality forecasting system for the Pacific Northwest was carried out for the 2007 and 2008 fire seasons using suite of surface and satellite observations. Wildfire events in the Pacific Northwest during the summers of 2007 and 2008 were simulated using the Air Information Report for Public Access and Community Tracking v.3 (AIRPACT-3) framework utilizing the Community Multi-scale Air Quality (CMAQ) model. Fire emissions were simulated using the BlueSky framework with fire locations determined by the Satellite Mapping Automated Reanalysis Tool for Fire Incident Reconciliation (SMARTFIRE). Plume rise was simulated using two different methods: the Fire Emission Production Simulator (FEPS) and the Sparse Matrix Operator Kernel Emissions (SMOKE) model. Predicted plume top heights were compared to the Cloud-Aerosol LIDAR with Orthogonal Polarization (CALIOP) instrument aboard the Cloud Aerosol LIDAR and Infrared Pathfinder Satellite Observation (CALIPSO) satellite. Carbon monoxide predictions were compared to the Atmospheric InfraRed Sounder (AIRS) instrument aboard the Aqua satellite. Horizontal distributions of column aerosol optical depth (AOD) were compared to retrievals by the Moderate Resolution Imaging Spectroradiometer (MODIS) instrument aboard the Aqua satellite. Model tropospheric nitrogen dioxide distributions were compared to retrievals from the Ozone Monitoring Instrument (OMI) aboard the Aura satellite. Surface ozone and $PM_{2.5}$ predictions were compared to surface observations. The AIRPACT-3 model captured the location and transport direction of fire events well, but sometimes missed the timing of fire events and overall underestimated the impact of wildfire events at regional surface monitor locations. During the 2007 fire period the fractional biases of AIRPACT-3 for average 24 h $PM_{2.5}$, maximum daily average 8 h Ozone, AOD, total column CO, and tropospheric column NO_2 were found to be −33 %, −8 %, −61 %, −10 %, and −39 %, respectively; while during the 2008 fire period the fractional biases were −27 %, +1 %, −53 %, −5 %, and −28 %, respectively. Fractional biases of AIRPACT-3 plume tops were found to be −46 % above mean sea level (a.m.s.l.), but only −28 % above ground

ACPD

14, 11103–11152, 2014

Air quality simulations of wildfires in the Pacific Northwest

F. L. Herron-Thorpe et al.

level (a.g.l.), partly due to the under-estimation of AIRPACT-3 elevation in complex terrain that results from the 12 km grid-cell smoothing.

1 Introduction

1.1 Motivation

The Pacific Northwest is home to forested lands that periodically experience large wildfires, especially during dry summers. Wildfire smoke and other particulate matter (PM) emitted into the atmosphere can cause severe respiratory problems. Alerting the public of poor air quality from fires requires a comprehensive knowledge of fire locations, land type being burned, terrain, wind direction, available moisture, timing, and other conditions. Reports generated by fire fighters are quickly provided to air quality managers by the United States Forest Service (USFS), but it is difficult to get an accurate assessment of wildfire conditions in remote locations with rough terrain, few access roads, and sparse air quality monitor distribution. Meteorological forecasts and air quality models can be used to predict the potential health impacts of wildfire emissions, but unfortunately there are many complexities involved with accurately predicting PM (Simon et al., 2012). Satellite retrievals of air quality provide a valuable asset that, when combined with surface measurements, can help to assess the validity of air quality models simulating large wildfire events. The analysis presented here utilizes multiple satellite products to evaluate simulations from the Air Information Report for Public Access and Community Tracking v.3 (AIRPACT-3) regional air quality model, which utilizes the BlueSky fire emissions framework and the Community Multi-scale Air Quality (CMAQ) model, for large wildfire events during the summers of 2007 and 2008. As such, this work demonstrates how a suite of satellite products can be combined with ground monitor observations to inform improvement of air quality forecast performance. The objective of this work is to report the level of performance and types of error that were found for modeled fire locations, plume heights, and pollutant concentrations simulated in AIRPACT-3 based on a combination of satellite products and surface pollutant observations.

1.2 Fire activity of 2007 and 2008

The western United States (US) experienced abnormally dry winter and spring seasons in 2007, which led to a summer drought and extensive wildfire events in Idaho, Nevada, and Montana. Extreme temperatures and sparse precipitation during early summer 2007, coupled with lightning activity and several strong wind events, led to several expanding, long-lived fires. Precipitation events that started on 17 August slowed the expansion of wildfires and allowed fire-fighters to contain many of the burning areas, though some fires continued to burn into September. The National Interagency Coordination Center (NICC) at the National Interagency Fire Center (NIFC; http://www.predictiveservices.nifc.gov/) reported that over 800 000 acres burned in Nevada during July 2007. By 31 August the Great Basin and Northern Rockies had wildfires that burned over 4 million acres, nearly twice the typical year-to-date area burned, with eight large fires or complexes having burned more than 100 000 acres each.

The summer of 2008 was also dry but experienced significantly less fire activity across the US, except for California and parts of the south. Northern California, part of which is in the AIRPACT-3 domain, reported over 850 000 acres burned, which was nearly 9 times the 10 year average for that region. On 20–21 June 2008, widespread lightning started nearly one thousand fires in northern California and those in remote and difficult terrain burned for many days. Lightning storms in mid-August 2008 also caused numerous large fires in Idaho and Montana. The number of acres burned by state reported by the NICC NIFC is shown in Table 1a for 2007 and 2008. Analysis of O_3 and particulate matter enhancements at the Mt. Bachelor Observatory (MBO) by Wigder et al. (2013) identified 14 individual fire plumes in 2008 and 6 in 2007.

The analysis presented here includes results for two separate time periods: 3 July–22 August 2007 and 22 June–27 August 2008, which were chosen to include the largest annual fire events in the AIRPACT-3 domain. There were several fires ignited on 6 July 2007 that led to 3 very large events: the Egley Complex in Oregon; the East Zone Complex in Idaho; and the Rattlesnake Complex in Idaho. There was another set of ignitions on 16 July 2007 that led to many very large fires: the Murphy Complex in Idaho and Nevada, which included the Winecup and Wildhorse complexes; the Cascade Complex in Idaho; and the Hepworth Complex in Nevada. Another set of fires was ignited in Idaho and Montana between 29 July and 2 August: the Shower Bath Complex; the Chippy Creek Fire; the Sawmill Complex; the Fool Creek Fire; the Jocko Lakes Fire; and the Brush Creek Fire. The 2008 analysis period was not as spatially dynamic as 2007 but was largely affected by several fires ignited on 21 June 2008 in Northern California that led to very large events that burned for several months in the Shasta-Trinity National Forest, Klamath National Forest, and surrounding areas: the Iron-Alps Complex burned, the Lime Complex, the Klamath Theater Complex, and the Shu Lightning Complex. Additional details about each reported fire complex that burned during the analysis period are given in Table 1b. Fire events during the analysis periods that included at least one reported fire over 5000 acres of burn area are shown in Fig. 1.

2 Methods

2.1 AIRPACT-3 air quality modeling system

The AIRPACT-3 modeling system (Chen et al., 2008; Herron-Thorpe et al., 2010, 2012) simulates air quality in the Pacific Northwest with the CMAQ v4.6 model (Byun and Schere, 2006). Area and non-road mobile emissions are from the 2002 Environmental Protection Agency (EPA) National Emissions Inventory (NEI), projected to 2005 using the EPA's Economic Growth Analysis System (EGAS) software; on-road mobile emissions are based on the EPA MOBILE v6.2 vehicle emission modeling software; anthropogenic emissions over Canada are from the 2000 Greater Vancouver Regional District

ACPD
14, 11103–11152, 2014

(GVRD) inventory; and biogenic emissions are obtained from the Biogenic Emissions Inventory System version 3 (BEIS-3). The AIRPACT-3 base emissions are processed using the Sparse Matrix Operator Kernel Emissions (SMOKE) v2.4 model while all fire emissions are processed with the SMOKE v2.7 model. The AIRPACT-3 domain includes a 95 × 95 grid of 12 km × 12 km cells using 21 layers from the surface to the lower stratosphere. The version of CMAQ used includes the Statewide Air Pollution Research Center (SAPRC) chemical mechanism (SAPRC-99), the ISORROPIA inorganic aerosol equilibrium module, and the Secondary Organic Aerosols Model (SORGAM). Meteorology inputs for AIRPACT-3 were derived from forecasts by Mass and colleagues (http://www.atmos.washington.edu/mm5rt/; Mass et al., 2003) and preprocessed for CMAQ using the AIRPACT-3 Meteorology Chemistry Interface Processor (MCIP). The Mesoscale Model v5 (MM5; Mass et al., 2003) was used for the year 2007 simulations while the Weather Research and Forecasting (WRF; Skamarock et al., 2005) model was used for the year 2008 simulations. Model of OZone And Related Tracers, version 4 (MOZART-4; Emmons et al., 2010) simulations produced at the National Center for Atmospheric Research (NCAR) were used as boundary conditions around the AIRPACT-3 domain (Emmons et al., 2010; Herron-Thorpe et al., 2012). The MOZART-4 simulations included the assimilation of satellite CO column v4 retrievals from the Measurement Of Pollution In The Troposphere (MOPITT) instrument, a gas-correlation radiometer on-board the National Aeronautics and Space Administration (NASA) Terra satellite (Deeter et al., 2010). The MOZART-4 emissions are the same as those used in Wespes et al. (2012), which include anthropogenic emissions based on the inventory developed by D. Streets for the NASA Arctic Research of the Composition of the Troposphere from Aircraft and Satellites (ARCTAS) experiment (http://bio.cgrer.uiowa.edu/arctas/emission.html) and biomass burning emissions from the Fire INventory of NCAR (FINN; Wiedinmyer et al., 2011).

Fire location, area, and emissions were calculated using BlueSky v3.1 data (http://www.airfire.org/bluesky), which utilizes USFS ICS-209 reports and hotspot detects reported by the Hazard Mapping System (HMS) together in the Satellite Mapping Au-

ACPD
14, 11103–11152, 2014

tomated Reanalysis Tool for Fire Incident Reconciliation (SMARTFIRE; Larkin et al., 2009; Raffuse et al., 2009). SMARTFIRE does well reporting wildfire location (Larkin et al., 2009; Strand et al., 2012), but is ultimately limited by the accuracy and completeness of the satellite detects and USFS reports filed. The fire reports used in this analysis are from the final SMARTFIRE archive, as distinct from the information reported in near real-time, which can often be incomplete.

For this analysis, the BlueSky framework (Larkin et al., 2009; Raffuse et al., 2009) was operated in default mode, which includes the use of the Consume v3 (Ottmar et al., 2009), Fuel Characteristic Classification System v1 (FCCS; Riccardi et al., 2007), and Fire Emission Production Simulator v1 (FEPS; Anderson et al., 2004) software programs provided by the USFS. FCCS v1 provides vegetation type and corresponding fuels (Fig. 1) at 1 km resolution, which is used as input to Consume. Consume then passes fuel consumption and emissions by combustion phase (smoldering or flaming) data to FEPS, which provides individual pollutant emissions, plume height, and the daily temporal profile. The default behavior of BlueSky classifies fuels as "dry", unless otherwise reported by SMARTFIRE. The result is that most of the grass and short-lived dead woody fuels are consumed in the simulations, but only 60 % of canopy fuels are consumed. This can result in large over-predictions during smaller events but can also lead to under-predictions during extreme conditions.

Two plume rise methods were used in this analysis, resulting in two sets of AIRPACT-3 model results. The first method uses the SMOKE-ready files created by BlueSky, which include hourly information, to explicitly set the plume rise to what FEPS predicts. The second set of model simulations were performed using methods that bypassed the FEPS plume rise algorithm and instead converted standard BlueSky output to create daily input files for SMOKE. It is important to note that the two plume rise methods used are based upon the same heat flux and smoldering/flaming emissions ratios but results differ in two ways: (1) whereas FEPS plume rise method allocates all smoldering emissions to the surface layer, the SMOKE plume rise method allows for smoldering emissions to be allocated throughout multiple layers near the surface; and (2) whereas

ACPD
14, 11103–11152, 2014

FEPS plume rise method does not utilize meteorology or surface elevation when predicting flaming plume heights, the SMOKE plume rise method computes flaming plume heights as a function of buoyancy using the heat content predicted by BlueSky, modeled meteorology, and modeled terrain heights (Pouliot et al., 2005).

2.2 AQUA-MODIS Aerosol Optical Depth (AOD)

The Aqua satellite was launched in May 2002 carrying the Moderate Resolution Imaging Spectroradiometer (MODIS) as part of NASA's Afternoon-Train (A-Train) of Earth Observing Satellites (EOS). The Aqua-MODIS retrievals provide aerosol information at nearly the same time as the other A-Train instruments, allowing coincident multi-species analyses, as presented in this analysis. MODIS reliably retrieves AOD for most of the globe on a daily basis with a nadir footprint of 10 km. Algorithms described by Remer et al. (2005) are used to interpolate the 470 nm and 660 nm retrievals to provide a 550 nm AOD product (MYD04_L2 v5.1). Typical AOD values at a clean site are below 0.3, while values over 1.0 are indicative of multiple scattering caused by high aerosol loading (i.e. heavy haze, biomass burning, or dust events). The maximum AOD values historically retrieved by MODIS are ~ 5.0, but these are rare events. Sources of error in MODIS AOD retrievals can include unique aerosol composition, varied land cover color, cloud fringes, and snow cover at high elevations (Levy et al., 2007; Drury et al., 2008). All MODIS AOD retrievals used in this analysis were re-gridded to the AIRPACT-3 grid by using the pixel with the closest proximity to the center of each AIRPACT-3 grid-cell. AIRPACT-3 grid-cells that did not have spatially corresponding high-quality MODIS retrievals were omitted from the analysis.

AIRPACT-3-simulated aerosol distributions were generated for all modeled aerosol species: nitrates, sulfates, ammonium, elemental carbon (EC), organic particulates, and coarse mode aerosols. AOD was calculated from AIRPACT-3 simulated aerosol species concentrations and size distributions using algorithms developed by Binkowski and Roselle (2003). This method uses the simulated aerosol total volume concentration V for the Aitken and accumulation mode aerosols and their associated Mie extinction

ACPD
14, 11103–11152, 2014

efficiency factors, Q_{ext}, to calculate AOD per modeled layer as described in Eq. (1), which is then integrated through the troposphere (layers 1–18) to yield the reported model AOD. An accurate approximation method from Evans and Fournier (1990) was used to calculate Q_{ext}.

$$\mathrm{AOD}_{\mathrm{layer}} = \frac{1000}{\lambda_{550\,\mathrm{nm}}}\left\{V_{[\mathrm{Aitken}]} \times Q_{\mathrm{ext}[\mathrm{Aitken}]} + V_{[\mathrm{accumulation}]} \times Q_{\mathrm{ext}[\mathrm{accumulation}]}\right\} + 0.01 \tag{1}$$

2.3 AIRS CO

In addition to MODIS, the Aqua satellite includes the Atmospheric Infra-Red Sounder (AIRS), which provides information about weather and trace gases. The AIRS instruments are an infrared spectrometer and a visible light/near-infrared photometer. The AIRS level-2 v5 product used in this analysis (AIRX2RET) provides carbon monoxide reported on the AMSU ground footprint, which varies from 36 km × 36 km to 50 km × 50 km. AIRS level-2 v5 data includes 7 trapezoidal layers of CO mixing ratio in the troposphere and an averaging kernel matrix for the full 9-layer profile available in the support product files. In this study the AIRPACT-3 profiles were convolved with the AIRS averaging kernels as discussed in Olsen et al. (2007) and Maddy and Barnet (2008), and then both were interpolated to the original AIRPACT-3 projection using a Delaunay triangulation scheme. In general, the AIRS averaging kernel slightly reduces the AIRPACT-3 total column CO, with some loss of information in the lower troposphere and enhanced middle troposphere sensitivity (Herron-Thorpe et al., 2012).

2.4 OMI tropospheric NO_2

The Aura satellite successfully joined the A-Train in July 2004, carrying multiple instruments that retrieve information about atmospheric chemistry. Tropospheric NO_2 columns retrieved by the Ozone Monitoring Instrument (OMI) are provided by the Tropospheric Emission Monitoring Internet Service (TEMIS; http://www.temis.nl/airpollution/no2.html). The Derivation of OMI tropospheric NO_2 (DOMINO) algorithms

ACPD
14, 11103–11152, 2014

calculate air mass factors (AMF), a priori profiles, stratospheric NO_2, and ghost columns from the daily global Tracer Model v4 (TM4), which is driven with meteorological fields from the European Centre of Medium-Range Forecasts (ECMWF) (Boersma et al., 2011). The product provides tropospheric NO_2 column retrievals with a 13 km × 24 km footprint at nadir with increasing footprint size as the observation moves off-nadir. A pixel's "ghost column" (below cloud) is estimated from the a priori profile for the pixel and OMI's retrieval of NO_2 above the cloud cover pressure level, with vertical sensitivity defined by the averaging kernel. The sum of the OMI ghost column and tropospheric column can be compared to a model column for an estimate of model performance. However, when the model NO_2 profile is convolved with the averaging kernel, the ghost column is no longer required.

Since OMI's NO_2 averaging kernel shows decreasing sensitivity as the vertical profile approaches the surface, the result of applying the averaging kernel to AIRPACT-3 NO_2 allows for essentially a "free troposphere" comparison with OMI. In this study we used OMI pixels with low cloud fraction (< 35 %) and convolved all AIRPACT-3 profiles with the OMI averaging kernel. AIRPACT-3 cells that fall within the spatial boundaries of each OMI pixel were averaged and interpolated, effectively reducing the resolution of the model results to equal that of the co-located OMI pixel, and then both were interpolated to the original AIRPACT-3 projection using a Delaunay triangulation scheme. This method works well for most areas but can lead to inconsistencies over areas with complex terrain (Herron-Thorpe et al., 2010).

2.5 CALIOP aerosol detection

The Cloud Aerosol LIDAR and Infrared Pathfinder Satellite Observation (CALIPSO) satellite successfully joined the A-Train in April 2006, carrying the Cloud-Aerosol LIDAR with Orthogonal Polarization (CALIOP) instrument as its main payload. CALIOP transmits a linearly polarized laser pulse and then detects the light that is reflected back. Determining the aerosol type from this space-based LIDAR depends on the attenuated backscatter, altitude, location, surface type, and the volume depolarization (ratio of the perpendicular backscatter to the parallel backscatter of the laser light retrieved). CALIPSO data were obtained from the NASA Langley Research Center Atmospheric Science Data Center. The CALIOP level-2 Vertical Feature Mask (VFM) data (v3.01) includes seven aerosol classes: clean marine, dust, polluted continental, clean continental, polluted dust, and smoke. Information about using the aerosol VFM product, including the relationship between horizontal resolution and elevation, was obtained from the CALIPSO Users Guide (http://www-calipso.larc.nasa.gov/resources/calipso_users_guide/). The horizontal and vertical resolutions of CALIOP are much finer than the AIRPACT-3 grid, but the instrument has very limited horizontal spatial coverage, with usable daytime overpasses only available approximately weekly. More details about CALIOP validation and selection algorithms used to classify aerosols are discussed by Liu et al. (2005), Mielonen et al. (2009), and Winker et al. (2009).

A VFM curtain was derived from the AIRPACT-3 simulated aerosol distributions using categories loosely based on information from Seinfeld and Pandis (1998). AIRPACT-3 pixels where $PM_{2.5}$ was greater than $3\,\mu g\,m^{-3}$ were categorized as the following aerosol types: "smoke" where over half the $PM_{2.5}$ mass was elemental carbon, "dust" if not "smoke" and over 20 % of aerosol mass was coarse mode, and "continental" if not "dust" nor "smoke". "Polluted" aerosol types were attributed to pixels not "smoke" if $PM_{2.5}$ was over $10\,\mu g\,m^{-3}$. The vertical curtains of simulated aerosol species were compared to coincident CALIOP retrievals to assess aerosol subtype performance. In addition, the plume top heights of pixels with a VFM aerosol subtype were compared for matched instances where both CALIOP and AIRPACT-3 data showed an aerosol subtype. Plume top heights were evaluated above mean sea-level (a.m.s.l.) and above ground-level (a.g.l.), so that discrepancies in terrain height could be evaluated. For this analysis, we consider a.g.l. plume heights to be relative to the ground level reported by the respective dataset.

ACPD
14, 11103–11152, 2014

2.6 Daily remote sensing activity

In addition to the methods described above, we also assessed overall fire conditions using MODIS true-color imagery of smoke plumes with markers for hot-spot locations, available from the Land Atmosphere Near Real-time Capability for EOS (LANCE; USA subset 1; http://lance-modis.eosdis.nasa.gov/imagery/subsets/index.php?project=fas). A daily remote sensing log of the LANCE-MODIS imagery and corresponding remote sensing comparisons, derived from the AIRPACT-3 FEPS plume-rise scenario, are available in the Supplement (Supplement Tables 1–4). Each fire region that was significantly over the signal-to-noise threshold was counted and tallied in the daily remote-sensing log for AOD and tropospheric NO_2 comparisons. AIRS resolution did not allow us to identify "distinguishable events" and were not tallied. For the purposes of this count, distinguishable fire regions could range from single large isolated fires to sizable areas with numerous fire locations, each of which have no overlapping transport from a remote sensing frame of reference.

2.7 Model performance statistics and ground-site selection

Definitions of the model performance statistics used are shown in Table 2. In order to avoid spurious results in the statistical calculations, all instances where negative values were reported by satellite products were screened, and very small AOD values were set to a minimum of 0.01. The ground-site analysis presented here uses combinations of 140 US surface monitor locations where AIRPACT-3 predicted more than double the normal surface $PM_{2.5}$, as a result of wildfire emissions. Surface monitor datasets that were excluded from the analysis had one or more of the following problems: no quality-controlled dataset was available, the site was primarily indicative of urban emissions, the site was in Canada where AIRPACT-3 has no wildfire emissions, or the site exhibited no distinguishable increase in surface $PM_{2.5}$ during fire events. The 2007 analysis period had 67 qualified $PM_{2.5}$ sites and 10 qualified ozone sites; while the 2008 analysis period had 82 qualified $PM_{2.5}$ sites and 18 qualified ozone sites.

ACPD
14, 11103–11152, 2014

The primary analysis of AOD, tropospheric column NO_2, and total column CO includes all 140 site locations. A secondary rural-sites-only subset includes 43 locations with no influence from transported urban pollution in the remote sensing record. This rural-sites-only subset is used for the "matched-threshold" analysis to help determine model performance for fire-polluted cases by only including instances where AIRPACT-3 and the monitor/retrieval in question both surpassed a threshold value: $10\,\mu g\,m^{-3}$ for the average 24 h surface $PM_{2.5}$, 0.3 for AOD, 1.0×10^{15} molecules cm^{-2} for tropospheric column NO_2, and 1.9×10^{18} molecules cm^{-2} for total column CO.

All surface monitor comparisons in this analysis were made using hourly data from the EPA Air Quality System (http://www.epa.gov/ttn/airs/airsaqs/detaildata/downloadaqsdata.htm), except for data from MBO in the Oregon Cascade mountains, which is not an AQS reporting site. MBO has been used to collect air quality data since 2004, including near-continuous observations of CO, O_3, aerosol scattering and meteorological parameters, and various other chemical species during intensive campaigns. MBO is located at coordinates 43.98° N, 121.69° W at an elevation of 2.7 km. The site has been used to investigate long-range transport of Asian pollution and biomass burning, regional wildfires, and other events including stratospheric intrusions (Weiss-Penzias et al., 2006; Ambrose et al., 2011; Wigder et al., 2013). AIRPACT-3 $PM_{2.5}$ and carbon monoxide concentrations were extracted from the layer corresponding to a height of 2.7 km in the model for comparisons to MBO to account for the discrepancy in model surface height. More details about the sites used, including elevation and location, can be found in Supplement Fig. 1.

3 Results

3.1 AIRPACT-3 compared to AIRS, MODIS, and OMI (3 July–22 August 2007)

Remote sensing of atmospheric gases and aerosols is limited by cloud conditions and the source signal strength at the relevant infrared/visible/UV wavelengths. Maps of

ACPD
14, 11103–11152, 2014

AOD, tropospheric NO_2 column, and total carbon monoxide column for analysis days in 2007 with favorable remote-sensing conditions are shown in Figs. 2–4. AIRPACT-3 under-predicted the impact of fires on AOD in Montana, W. Idaho, S. Idaho, and Nevada on 22 July (Fig. 2 and Supplement Fig. 5). AIRPACT-3 also under-predicted tropospheric column NO_2 in Nevada and Montana on 22 July, but the largest modeled fires were not observed via remote sensing, in central Idaho near the Montana border, likely due to mis-match in timings of fire emissions and satellite detections. 12 August (Fig. 3 and Supplement Fig. 6) and 18 August (Fig. 4 and Supplement Fig. 7) show typical AIRPACT-3 performance during the largest fire periods in 2007. Fire locations and intensity were predicted well in Idaho and Montana but AIRPACT-3 over-predicted total column CO and AOD in Montana. AIRPACT-3 did not predict the observed fire impacts in Nevada that were transported from south of the domain.

The Daily Remote Sensing Log for 2007 (Supplement Table 1) notes that there were 44 days in the 2007 period analyzed that confidently showed MODIS AOD from fires: of the 176 total discernible events, 8 % were observed but not predicted, 37 % were under-predicted, 30 % were predicted well, 20 % were over-predicted, and 5 % were predicted but not observed. We found that the magnitude of predicted AOD that extended to large distances from sources inside the domain was under-predicted for 13 % of discernible events. Additionally, we found that the magnitude of predicted AOD from sources outside the domain was under-predicted during 8 of the 44 days. There were also 2 days where MODIS AOD clearly showed aerosol loading retained from the previous day that were not predicted.

The Daily Remote Sensing Log for 2007 (Supplement Table 2) also notes that there were 31 days in the 2007 period analyzed that confidently showed tropospheric NO_2 from fires: of the 122 total discernible events, 0 % were observed but not predicted, 23 % were under-predicted, 21 % were predicted well, 48 % were over-predicted, and 8 % were predicted but not observed.

Overall, AIRPACT was under-biased for all analyzed pollutants from 3 July to 23 August 2007. In comparison, for non-fire periods across the whole domain, AIRPACT

ACPD
14, 11103–11152, 2014

tends to over-estimate $PM_{2.5}$ levels by ∼ 3 % (Chen et al., 2008). The fractional biases of the SMOKE plume rise scenario for AOD, tropospheric column NO_2, and total column CO for all 140 sites were −61 %, −39 %, and −10 %, respectively. The FEPS plume rise scenario changed results by a few percent with fractional biases of −66 %, −38 %, and −13 %, respectively (Table 3). In comparison, the fractional biases for the matched-threshold analysis of the SMOKE plume rise scenario for all 43 rural sites were −101 %, −98 %, and −10 %, respectively. The fractional biases for the matched-threshold analysis of the FEPS plume rise scenario were −117 %, −97 %, and −18 %, respectively (Table 4).

3.2 AIRPACT-3 compared to AIRS, MODIS, and OMI (22 June–27 August 2008)

Examples of AOD, tropospheric NO_2 column, and total carbon monoxide column maps are shown for days in 2008 with favorable remote sensing conditions in Figs. 5–7 for 29 June, 11 July, and 20 July respectively (also see Supplement Figs. 8–10). Figure 5 shows that AIRPACT-3 under-estimated the fire-generated pollutants from N. California on 29 June and missed pollutants transported from outside of the domain. Figure 6 shows that AIRPACT-3 did better predicting fires in N. California on 11 July, but continued to miss fire-generated pollutants from outside of the domain. This is especially evident in Nevada where fire-generated AOD originating from south of the AIRPACT-3 domain was observed but not predicted. This suggests that boundary conditions derived from the MOZART-4 simulations under-predict the influence of fires from outside the domain.

AIRPACT did well predicting an interesting transport case on 20 July, but over-predicted the near-source pollutants in N. California/S. Oregon while under-predicting the transported aerosol from within the domain and over-predicting the transported CO from within the domain (Fig. 7). In general, AIRPACT-3 had difficulty accurately predicting aerosols that originated over ∼ 100 km from the source during large fire plume events. A timeline of events in July and August of 2008 that transported fire-

ACPD
14, 11103–11152, 2014

generated pollutants, which were detected at Mt. Bachelor Observatory, are discussed in Sect. 3.8.

The Daily Remote Sensing Log for 2008 (Supplement Tables 3) notes that there were 64 days in the 2008 period analyzed that confidently showed AOD from fires: of the 108 discernible events, 6 % were observed but not predicted, 32 % were under-predicted, 31 % were predicted well, 18 % were over-predicted, and 13 % were predicted but not observed. We found that the magnitude of predicted AOD transported large distances from sources inside the domain was under-predicted for 31 % of discernible events. Additionally, we found that the magnitude of predicted AOD from sources outside the domain was under-predicted during 27 of the 64 days. There were also 3 days (1, 6, 11 July) where MODIS AOD clearly showed aerosol loading retained from the previous day that were not predicted.

The Daily Remote Sensing Log for 2008 (Supplement Table 4) also notes that there were 44 days in the 2008 period analyzed that confidently showed tropospheric NO_2 from fires: of the 76 discernible events, 4 % were observed but not predicted, 13 % were under-predicted, 30 % were predicted well, 37 % were over-predicted, and 16 % were predicted but not observed. There was also 1 day (1 July) where OMI clearly showed tropospheric NO_2 loading retained from the previous day that was not predicted.

Overall, AIRPACT was biased low for all analyzed pollutants from 22 June to 27 August 2008. The fractional biases of the SMOKE plume-rise scenario for AOD, tropospheric column NO_2, and total column CO for all 140 sites were −53 %, −28 %, and −5 %, respectively. The FEPS plume rise scenario changed results by a few percent, with fractional biases of −58 %, −26 %, and −7 %, respectively (Table 5). In comparison, the fractional biases for the matched-threshold analysis of the SMOKE plume rise scenario for all 43 rural sites were −105 %, −93 %, and −9 %, respectively. The fractional biases for the matched-threshold analysis of the FEPS plume rise scenario were −125 %, −90 %, and −12 %, respectively (Table 6).

ACPD
14, 11103–11152, 2014

3.3 AIRPACT-3 vs. CALIPSO plume top and aerosol subtype

CALIOP retrievals were compared to AIRPACT aerosols across the model domain when CALIPSO passed over the Idaho and California wildfire smoke plumes during the analysis periods of 2007 and 2008, respectively. There were many instances where both AIRPACT-3 and CALIOP showed the presence of fire-related aerosol pollution at similar heights. In 2007, CALIOP retrievals showed aerosol pollution over 328 unique AIRPACT grid cells (across Nevada, Idaho, and Canada), while 218 and 219 of those grid cells had AIRPACT-3 aerosol pollution in the SMOKE and FEPS plume rise scenarios, respectively, as determined by the chosen thresholds described in Sect. 2.5. In 2008, CALIOP retrievals showed aerosol pollution over 383 unique AIRPACT grid cells (across California, Oregon, Washington, and Canada), while 281 and 275 of those grid cells had AIRPACT-3 aerosol pollution in the SMOKE and FEPS plume rise scenarios, respectively, past the chosen thresholds.

There was moderate linear correlation (r^2 = 0.41 for FEPS plume rise; r^2 = 0.50 for SMOKE plume rise) between AIRPACT-3 and CALIPSO plume top heights a.m.s.l., when both showed the presence of an aerosol subtype. On average, the AIRPACT-3 FEPS plume-rise scenario under-predicted plume top heights a.m.s.l. by 3.1 ± 2.3 km in 2007 and 2.5 ± 1.5 km in 2008, while the SMOKE plume-rise scenario under-predicted plume top heights a.m.s.l. by 3.1 ± 2.0 km in 2007 and 2.2 ± 1.6 km in 2008 (Fig. 8). There were many instances with similar plume heights, relative to terrain, but dissimilar terrain heights resulted in large under-predictions in plume top heights a.m.s.l.. The horizontal resolution of AIRPACT smoothes the surface elevation in complex terrain so that it is consistently lower relative to CALIOP retrievals, and is a large source of uncertainty when assessing AIRPACT plume top performance. We found less linear correlation (r^2 = 0.18 for FEPS plume rise; r^2 = 0.24 for SMOKE plume rise) between AIRPACT-3 and CALIPSO plume tops heights a.g.l., when both showed the presence of aerosol subtype. On average, though, the AIRPACT-3 FEPS plume-rise scenario under-predicted plume top heights a.g.l. by 1.4 ± 2.3 km in 2007 and 1.0 ± 1.2 km in

2008 while the SMOKE plume-rise scenario under-predicted plume top heights a.g.l. by 1.5 ± 1.9 km in 2007 and 0.9 ± 1.3 km in 2008 (Fig. 8). More information about the CALIOP plume top comparison is shown in Table 7. This is consistent with a national study using a similar modeling structure, where CMAQ plume heights were under-predicted by ~ 20 %, relative to CALIOP retrievals (Raffuse et al., 2012).

We found that aerosol subtype reported by CALIOP was very dynamic within each fire plume, with many occurrences of smoke and polluted dust combined with occasional occurrences of the other aerosol subtypes. On the other hand, AIRPACT-3 predicted the majority of fire plumes as "smoke", with portions of plumes occasionally categorized as "clean continental". We recognize that the CALIOP VFM subtype does well identifying dust, fine aerosols include large uncertainties inherent to the method (Mielonen et al., 2009), which make it difficult to evaluate AIRPACT aerosol subtypes using the CALIOP VFM retrieval.

3.3.1 Surface concentration results (3 July–22 August 2007)

Daily 24 h average $PM_{2.5}$ was averaged across 67 sites and the maximum daily 8 h average ozone was averaged across 10 sites for modeled and measured concentrations from 3 July to 22 August 2007. The timeline that represents this domain-wide comparison (Fig. 9) shows that maximum daily 8 h surface ozone was generally under-predicted by 2–8 ppb, but AIRPACT-3 did predict general changes in ozone that were similar to what was observed. The timeline also shows that AIRPACT-3 generally under-predicted daily surface $PM_{2.5}$ averages by 2–5 $\mu g\,m^{-3}$ and followed the measured curve closely except for gross over-prediction of surface $PM_{2.5}$ concentrations from 14–16 August 2007.

3.3.2 Surface concentration results (22 June–27 August 2008)

Daily 24 h average $PM_{2.5}$ was averaged across 82 sites and the maximum daily 8 h average ozone averaged across 18 sites for modeled and measured concentrations from

22 June to 27 August 2008. The timeline that represents this domain-wide comparison (Fig. 9) shows that AIRPACT-3 maximum daily 8 h surface ozone concentrations followed the measured curve quite closely with occasional errors of only a few ppb. This timeline also shows that AIRPACT-3 generally predicted daily surface $PM_{2.5}$ averages within a few $\mu g\,m^{-3}$, but made very large over-predictions in the FEPS plume rise scenario during the 12–13 July 2008 fires.

3.4 Relevance to the $PM_{2.5}$ National Ambient Air Quality Standards (NAAQS)

The AIRPACT-3 daily 24 h $PM_{2.5}$ performance was assessed from a policy standpoint by calculating the number of days per station where the forecast system and the observations both showed a $PM_{2.5}$ concentration greater than the national standards. We tallied the number of these days during the analysis period, for 67 sites in 2007 and 82 sites in 2008, of both the annual ($12\,\mu g\,m^{-3}$) and daily ($35\,\mu g\,m^{-3}$) standard threshold values. For the $35\,\mu g\,m^{-3}$ threshold FEPS plume-rise scenario, on a per-site per-day basis: 97.7 % of the cases were less than the standard for both the forecast and observation, 0.2 % of the cases were higher than the standard for both the forecast and observation, 0.3 % of the cases were observed to be higher than the standard but was not predicted as such, and 1.8 % of the cases were predicted to be higher than the standard but were not observed as such. However, the SMOKE plume-rise scenario reduced the number of times the predictions were higher than the standard when it was not observed as such by 27 % (1.3 % of the cases). In comparison, for the $12\,\mu g\,m^{-3}$ threshold FEPS plume-rise scenario: 90.7 % of the cases were less than the standard for both the forecast and observation, 1.8 % of the cases were higher than the standard for both the forecast and observation, 4 % of the cases were observed to be higher than the standard but was not predicted as such, and 3.5 % of the cases were predicted to be higher than the standard but were not observed as such. For the $12\,\mu g\,m^{-3}$ threshold, the SMOKE plume-rise scenario increased the number of cases that were higher than the standard for both the forecast and observation by 17 % (2.1 % of the cases). Table 8 shows further details of the comparison of observed and predicted surface

ACPD
14, 11103–11152, 2014

concentrations, relative to the $PM_{2.5}$ NAAQS, separately for 2007 and 2008, while the location and numbers per site are shown for the FEPS scenario in Supplement Figs. 2 and 3, respectively.

3.5 2008 MBO analysis

Hourly observed and predicted AIRPACT-3 values for PM, carbon monoxide, and ozone at MBO during the 2008 California wildfires (Fig. 10) show how AIRPACT-3 generally does with medium-range transport of wildfire emissions. There is evidence of model under-prediction, especially in the FEPS plume-rise scenario, but the SMOKE plume-rise scenario resulted in over-prediction of CO for most fire events. There was generally good agreement of the timing of pollution events but occasionally the timing was off by a day, as occurred on 8–9 August (Fig. 10). Note that PM for AIRPACT-3 in the MBO analysis is reported as $PM_{2.5}$ but the observations are of sub-micron aerosols converted from scattering observations using the method described in Wigder et al. (2013).

On 20 July, there was a large transport event that carried pollutants northwest from the fires in California until reaching the coast of Oregon where the plume was diverted inland to the northeast, sweeping across Oregon (see Fig. 7 and Supplement Fig. 4). MBO measurements of sub-micron PM were between 80 and 120 $\mu g\,m^{-3}$ from midnight to noon, and between 20 and 45 $\mu g\,m^{-3}$ for the proceeding 24 h. AIRPACT-3 predictions of carbon monoxide and $PM_{2.5}$ were well timed with monitor observations, but the AIRPACT-3 FEPS plume-rise scenario consistently under-predicted CO and PM concentrations during the event while the SMOKE plume rise scenario did better on average but still under-predicted PM. The event did not have emissions from outside the domain that significantly contributed to the plume, but some aerosols were clearly lost to the domain boundary, unable to sweep back with the horizontal motion that occurred. However, there was not enough aerosol that the model transported out of the boundary to explain how the AIRPACT-3 SMOKE plume-rise scenario predicted carbon monoxide well but under-predicted PM by $\sim 50\,\%$ in the afternoon and $\sim 30\,\%$ through proceeding hours. There was a smaller event with similar comparisons between observations and

ACPD
14, 11103–11152, 2014

predictions on 25 July as well. Throughout the 2008 MBO analysis dates, AIRPACT-3 generally under-predicted aerosols when CO was predicted well and over-predicted CO when aerosols were predicted well. This is consistent with other observations that show AIRPACT-3 $PM_{2.5}$/CO ratios to be low at locations greater than ~ 100 km from the fire location. Observations on 20 July, 25 July, and 9 August resulted in PM_1/CO ratios of ~ 0.3 $\mu g\,m^{-3}\,ppbv^{-1}$, higher than the ratios observed for fires in closer proximity to MBO, which has been previously interpreted to indicate secondary organic aerosol (SOA) formation during plume transport (Wigder et al., 2013).

The remote sensing comparison of the unique event on 20 July confirmed a consistent negative bias in predicted transported aerosols, even where CO in the SMOKE plume-rise scenario agreed well with AIRS. MODIS observed AOD values as high as 1.2 directly northwest of MBO, with lower values near 0.4 directly over the site. AIRPACT-3 only predicted AOD of 0.1 to 0.4 through the region of the large plume over those same regions around MBO (Fig. 7). AIRS also retrieved good quality carbon monoxide columns west of MBO, in the more concentrated part of the plume, showing a model under-bias of ~ 10 %. Tropospheric NO_2 columns over the transported portion of the plume were below the signal to noise threshold of OMI.

MOZART-4 results are included in Fig. 10, as an evaluation of the boundary conditions used to drive AIRPACT-3. The global model results, interpolated to the MBO location, show general agreement with the background values of CO and O_3, but miss the higher values due primarily to the coarse model resolution, as well as a poor representation of the fire emissions.

4 Discussion

AIRPACT-3 correctly predicted which regions were impacted by fires in Idaho, Montana, Nevada, California, and Oregon during the summers of 2007 and 2008. This is reflected in the comparisons to AIRS carbon monoxide, OMI tropospheric NO_2, and MODIS AOD, which all exhibited good spatiotemporal correlation to AIRPACT-3. Model performance results were quite similar between the two years, which suggests that the differences from using MM5 in 2007 and WRF in 2008 did not have a significant effect on the chemical transport modeling during the fire events.

The SMOKE plume-rise scenario exhibited the best model performance, with average fractional biases at ∼ 2 p.m. for AOD, total column CO, and tropospheric column NO_2 found to be −61 %, −10 %, and −39 % during the 2007 fire period, respectively; while during the 2008 fire period the average fractional biases were −53 %, −5 %, and −28 %, respectively. Surface concentrations of $PM_{2.5}$ were also reasonable, especially in the SMOKE plume rise scenarios, which lifted some of the surface emissions aloft and constrained large plume top heights. The fractional bias of daily average 24 h $PM_{2.5}$ was found to be approximately −30 % during both fire periods. Fractional biases of AIRPACT-3 plume tops were found to be −46 % above mean sea level (a.m.s.l.), but only −28 % above ground level (a.g.l.), partly due to the under-estimation of AIRPACT-3 elevation in complex terrain. Underestimation of plume heights, which affects transport, may be partly responsible for under-prediction in transported aerosols. However, the under-prediction of SOA in model simulations is likely the largest source of model error, especially when we consider that other species, such as CO, were not under-predicted by such large magnitudes.

Fire emissions generated from south of the domain were not well represented in AIRPACT-3 boundary conditions derived from MOZART-4 and a few events in 2008 appeared to be significantly affected by those under-predictions in boundary condition concentrations. Thus model performance would benefit from new methods to better represent fire influence on AIRPACT-3 boundary conditions.

Comparisons of AIRPACT-3 plumes with CALIOP show that the dynamics of plume dispersion in the model are greatly affected by errors in surface terrain and vertical plume distribution and their interaction with the wind profiles. There is also evidence that the underestimation of terrain height in AIRPACT-3 and the overestimation of plume-top heights a.g.l. could be compensating errors in some of the FEPS plume rise scenarios.

ACPD
14, 11103–11152, 2014

AIRPACT-3 tropospheric NO_2 was generally under-predicted, but there were occasionally what appeared to be large overestimates of tropospheric NO_2 over active fire regions (Figs. 4 and 7). It is important to note that these large tropospheric NO_2 predictions shown are a direct result of our application of the OMI averaging kernel, which weights the upper troposphere with a factor greater than one. In most cases, the plumes are low enough to the ground that the averaging kernel causes a net reduction in AIRPACT-3 tropospheric NO_2 columns. However, in cases where FEPS considerably over-predicted plume top height, the modeled tropospheric NO_2 column convolved with the averaging kernel caused a spike much higher than that of the original AIRPACT-3 results. The effect still occurs in the SMOKE plume rise scenario, though there are fewer extreme instances. Furthermore, the OMI tropospheric NO_2 algorithms produce large errors when detecting wildfires because of the a priori profiles used that assume NO_2 is concentrated near the surface, the high aerosol loadings emitted, and issues with comparisons over complex terrain (Boersma et al., 2011). We feel that users of tropospheric NO_2 satellite retrievals would benefit from an alternative retrieval that uses a priori profiles more suitable for fire plume conditions.

AIRPACT-3 column CO was slightly under-predicted outside of the center of the transported plumes, but there were often similar estimates of column CO over active fire regions (Figs. 4, 5 and 7). The AIRS retrieval is not sensitive to the surface, but our analysis suggests that AIRPACT-3 often accurately predicts transported CO concentrations. This is in contrast to the frequent underestimates of transported aerosols that were evident in AIRPACT-3 predictions of AOD (Figs. 3–5 and 7).

The MBO analysis clearly shows that even when model emissions and transport of CO are in close agreement with observations, aerosol performance degrades with distance from the source. We believe this is largely due to an under-prediction of SOA in CMAQ, which can be a significant fraction of the total measured PM for plumes transported large distances (Wigder et al., 2013; Strand et al., 2012; Hu et al., 2008; Heilman et al., 2013).

ACPD
14, 11103–11152, 2014

Collectively, the results of this analysis show that AIRPACT-3 can over-predict surface fire emissions and occasionally under-predict fire emissions aloft which, coupled with discrepancies in modeled surface elevation, significantly affects the ability of AIRPACT-3 to accurately predict downwind surface concentrations of transported pollutants in complex terrain. In an attempt to address the negative bias of transported pollutants in AIRPACT-3, we also tested scenarios where all surface (smoldering) emissions were allocated to the plume (flaming) emissions. This "Smolder Emissions in Plume" scenario did address the over-predictions of surface concentrations near fire locations, but did not significantly affect performance at sites further downwind.

5 Conclusions and future work

In general, AIRPACT-3 over-predicts pollutant concentrations due to near-source surface emissions from fires and under-predicts concentrations associated with long-range transport both from within the domain and outside the domain. Most fire locations are captured by the BlueSky SMARTFIRE tool, but there are occasionally fires predicted that are poorly timed or are completely absent. Our analysis suggests that total emissions in the domain are, overall, modestly under-predicted. Although we have shown that AIRPACT-3 boundary conditions largely under-estimate fire-emissions from outside the domain, this problem does not explain most under-predictions that occur at ground sites. The under-predictions are instead likely due to a combination of some or all of the following: (1) missing fire locations in the SMARTFIRE feed, which is expected for some fires in complex terrain and covered by cloud or smoke; (2) underestimates of acres burned in the SMARTFIRE feed; (3) underestimates of fuel mass, especially in shrub-lands and other vegetation types that completely lack dead woody fuels in the FCCS classification; (4) under-predictions of SOA production in CMAQ, thus causing under-predictions of aerosols in plumes that travel large distances; and (5) terrain height in the AIRPACT-3 model is too smooth in mountainous areas, causing problems with the elevation of emissions and dynamics of transport. Under-predictions in emis-

ACPD
14, 11103–11152, 2014

sions also scale directly with under-predictions in plume top heights, which exacerbates model performance of events with large transport distances.

Given the results of this analysis and other BlueSky simulations tested, we have determined that AIRPACT-3 fire prediction performance would benefit by addressing the following concerns: (1) moisture parameters should be changed to be dynamic based on the location and season, (2) fuel data for Canada should be added so fires can be represented there, (3) the FCCS software should be upgraded to v2, which will increase resolution and give a better representation of fuels, (4) boundary condition methods are needed that provide more accurate representations of smoke originating from outside the AIRPACT domain, and (5) test newer chemistry and aerosol methods as they are available in CMAQ. In the future, updating the AIRPACT vertical layer spacing in the middle troposphere to include more layers should also help model performance during fire emissions transport events. Incorporating new systems such as the WRF-CMAQ coupling with aerosol feedback (Wong et al., 2012) may also increase aerosol performance, especially for long-range fire transport when SOA can be significant. Furthermore, we recognize that coupling fire dynamics with meteorological simulations, such as in the WRF-Fire framework (Coen et al., 2013; Kochanski et al., 2013; Mandel et al., 2011) will eventually become necessary to improve air quality predictions during wildfire seasons. In addition, satellite users could benefit from additional trace gas column retrieval products that are optimized for fire events.

Supplementary material related to this article is available online at http://www.atmos-chem-phys-discuss.net/14/11103/2014/acpd-14-11103-2014-supplement.pdf.

Acknowledgements. This research was made possible by a NASA grant (NNX11AE57G) and was also partially supported by a grant from the National Science Foundation's REU program (0754990). The National Center for Atmospheric Research is funded by the National Science Foundation and operated by the University Corporation for Atmospheric Research. The Mt. Bachelor Observatory is supported by the National Science Foundation (AGS-

1066032AM002). NW-AIRQUEST provides support for the operation of the AIRPACT forecast system.

References

Ambrose, J. L., Reidmiller, D. R., and Jaffe, D. A.: Causes of high O_3 in the lower free troposphere over the Pacific Northwest as observed at the Mt. Bachelor Observatory, Atmos. Environ., 45, 5302–5315, doi:10.1016/j.atmosenv.2011.06.056, 2011.

Anderson, G. K., Sandberg, D. V., and Norheim, R. A.: Fire Emission Production Simulator (FEPS) User's Guide, Joint Fire Science Program and the National Fire Plan, January, USDA Forest Service available at: http://www.fs.fed.us/pnw/fera/feps/FEPS_users_guide.pdf, 2004.

Bhoi, S., Qu, J. J., Dasgupta, S.: Multi-sensor study of aerosols from 2007 Okefenokee forest fire, J. Appl. Remote Sens., 3, 031501, doi:10.1117/1.3078070, 2009.

Binkowski, F. S. and Roselle, S. J.: Models-3 Community Multiscale Air Quality (CMAQ) model aerosol component, 1. Model description, J. Geophys. Res., 108, 4183, doi:10.1029/2001JD001409,2003.

Boersma, K. F., Eskes, H. J., Veefkind, J. P., Brinksma, E. J., van der A, R. J., Sneep, M., van den Oord, G. H. J., Levelt, P. F., Stammes, P., Gleason, J. F., and Bucsela, E. J.: Near-real time retrieval of tropospheric NO_2 from OMI, Atmos. Chem. Phys., 7, 2103–2118, doi:10.5194/acp-7-2103-2007, 2007.

Boersma, K. F., Eskes, H. J., Dirksen, R. J., van der A, R. J., Veefkind, J. P., Stammes, P., Huijnen, V., Kleipool, Q. L., Sneep, M., Claas, J., Leitão, J., Richter, A., Zhou, Y., and Brunner, D.: An improved tropospheric NO_2 column retrieval algorithm for the Ozone Monitoring Instrument, Atmos. Meas. Tech., 4, 1905–1928, doi:10.5194/amt-4-1905-2011, 2011.

Byun, D. and Schere, K. L.: Review of the governing equations, computational algorithms, and other components of the models-3 Community Multiscale Air Quality (CMAQ) modeling system, Appl. Mech. Rev., 59, 51–77, doi:10.1115/1.2128636, 2006.

Calipso User Guide: CALIPSO Lidar Level-2 5 km Vertical Feature Mask (VFM) Products, NASA Langley Research Center, available at: http://www-calipso.larc.nasa.gov/resources/calipso_users_guide/data_summaries/vfm/ (last access: 6 October 2011), 2011.

ACPD
14, 11103–11152, 2014

Air quality simulations of wildfires in the Pacific Northwest

F. L. Herron-Thorpe et al.

Chen, J., Vaughan, J., Avise, J., O'Neill, S., and Lamb, B.: Enhancement and evaluation of the AIRPACT ozone and $PM_{2.5}$ forecast system for the Pacific Northwest, J. Geophys. Res., 113, D14305, doi:10.1029/2007JD009554, 2008.

Christopher, S., Gupta, P., Nair, U., Jones, T. A., Kondragunta, S., Wu, Y.-L., Hand, J., and Zhang, X.: Satellite remote sensing and mesoscale modeling of the 2007 Georgia/Florida fires, IEEE J. Sel. Top. Appl., JSTARS-2009-00020, 26, 1–13, 2009.

Coen, J., Cameron, M., Michalakes, J., Patton, E., Riggan, P., and Yedinak, K.: WRF-Fire: coupled weather-wildland fire modeling with the weather research and forecasting model, J. Appl. Meteorol. Clim., 52, 16–38, doi:10.1175/JAMC-D-12-023.1, 2013.

Deeter, M. N., Edwards, D. P., Gille, J. C., Emmons, L. K., Francis, G., Ho, S. P., Mao, D., Masters, D., Worden, H., Drummond, J. R., and Novelli, P. C.: The MOPITT version 4 CO product: algorithm enhancements, validation, and long-term stability, J. Geophys. Res., 115, D07306, doi:10.1029/2009JD013005, 2010.

Drury, E., Jacob, D. J., Wang, J., Spurr, R. J. D., and Chance, K.: Improved algorithm for MODIS satellite retrievals of aerosol optical depths over western North America, J. Geophys. Res., 113, D16204, doi:10.1029/2007JD009573, 2008.

Emmons, L. K., Walters, S., Hess, P. G., Lamarque, J.-F., Pfister, G. G., Fillmore, D., Granier, C., Guenther, A., Kinnison, D., Laepple, T., Orlando, J., Tie, X., Tyndall, G., Wiedinmyer, C., Baughcum, S. L., and Kloster, S.: Description and evaluation of the Model for Ozone and Related chemical Tracers, version 4 (MOZART-4), Geosci. Model Dev., 3, 43–67, doi:10.5194/gmd-3-43-2010, 2010.

Engel-Cox, J. A., Holloman, C. H., Coutant, B. W., Hoff, R. M.: Qualitative and quantitative evaluation of MODIS satellite sensor data for regional and urban scale air quality, Atmos. Environ., 38, 2495–2509, doi:10.1016/j.atmosenv.2004.01.039, 2004.

Evans, T. N. and Fournier, G. R.: Simple approximation to extinction efficiency valid over all size range, Appl. Optics, 29, 4666–4670, 1990.

Green, M., Kondragunta, S., Ciren, P., Xu, C.: Comparison of GOES and MODIS Aerosol Optical Depth (AOD) to AErosol RObotic NETwork (AERONET) AOD and IMPROVE $PM_{2.5}$ mass at Bondville, Illinois, J. Air Waste Manage., 59, 1082–1091, doi:10.3155/1047-3289.59.9.1082, 2009.

Heilman, W. E., Liu, Y., Urbanski, S., Kovalev, V., and Mickler, R.: Wildland fire emissions, carbon, and climate: plume rise, atmospheric transport, and chemistry processes, Forest Ecol. Manage., 317, 70–79, doi:10.1016/j.foreco.2013.02.001, 2014.

ACPD

14, 11103–11152, 2014

Herron-Thorpe, F. L., Lamb, B. K., Mount, G. H., and Vaughan, J. K.: Evaluation of a regional air quality forecast model for tropospheric NO_2 columns using the OMI/Aura satellite tropospheric NO_2 product, Atmos. Chem. Phys., 10, 8839–8854, doi:10.5194/acp-10-8839-2010, 2010.
Herron-Thorpe, F. L., Mount, G. H., Emmons, L. K., Lamb, B. K., Chung, S. H., and Vaughan, J. K.: Regional air-quality forecasting for the Pacific Northwest using MOPITT/TERRA assimilated carbon monoxide MOZART-4 forecasts as a near real-time boundary condition, Atmos. Chem. Phys., 12, 5603–5615, doi:10.5194/acp-12-5603-2012, 2012.
Hoff, R. M. and Christopher, S. A.: Remote sensing of particulate pollution from space: Have we reached the promised land?, J. Air Waste Manage., 59, 645–675, 2009.
Hu, Y., Talat Odman, M., Chang, M. E., Jackson, W., Lee, S., Edgerton, E. S., Baumann, K., and Russell, A. G.: Simulation of air quality impacts from prescribed fires on an urban area, Environ. Sci. Technol., 42, 3676–3682, 2008.
Kahn, R. A.: Wildfire smoke injection heights: two perspectives from space, Geophys. Res. Lett., 35, L04809, doi:10.1029/2007GL032165, 2008.
Kochanski, A. K., Jenkins, M. A., Krueger, S. K., Mandel, J., and Beezley, J. D.: Real time simulation of 2007 Santa Ana fires, Forest Ecol. Manag., 15, 136–149, doi:10.1016/j.foreco.2012.12.014arXiv:1202.3209, 2013.
Larkin, N. K., O'Neill, S. M., Solomon, R., Raffuse, S., Strand, T., Sullivan, D. C., Krull, C., Rorig, M., Peterson, J., and Ferguson, S. A.: The BlueSky smoke modeling framework, Int. J. Wildland Fire, 18, 906–920, 2009.
Levy, R. C., Remer, L. A., Mattoo, S., Vermote, E. F., and Kaufman, Y. J.: Second-generation operational algorithm: retrieval of aerosol properties over land from inversion of moderate resolution imaging spectroradiometer spectral reflectance, J. Geophys. Res., 112, D13211, doi:10.1029/2006JD007811, 2007b.
Maddy, E. S. and Barnet, C. D.: Vertical resolution estimates in version 5 of AIRS operational retrievals, IEEE T. Geosci. Remote, 46, 2375–2384, doi:10.1109/TGRS.2008.917498, 2008.
Mandel, J., Beezley, J. D., and Kochanski, A. K.: Coupled atmosphere-wildland fire modeling with WRF 3.3 and SFIRE 2011, Geosci. Model Dev., 4, 591–610, doi:10.5194/gmd-4-591-2011, 2011.
Mass, C. F., Albright, M., Ovens, D., Steed, R., MacIver, M., Grimit, E., Eckel, T., Lamb, B., Vaughan, J., Westrick, K., Storck, P., Colman, B., Hill, C., Maykut, N., Gilroy, M., Ferguson, S. A., Yetter, J., Sierchio, J. M., Bowman, C., Stender, R., Wilson, R., and Brown, W.:

ACPD
14, 11103–11152, 2014

Air quality simulations of wildfires in the Pacific Northwest

F. L. Herron-Thorpe et al.

Regional environmental prediction over the Pacific Northwest, B. Am. Meteorol. Soc., 84, 1353–1366, 2003.
Mielonen, T., Arola, A., Komppula, M., Kukkonen, J., Koskinen, J., de Leeuw, G., and Lehtinen, K. E. J.: Comparison of CALIOP level 2 aerosol subtypes to aerosol types derived from AERONET inversion data, Geophys. Res. Lett., 36, L18804, doi:10.1029/2009GL039609, 2009.
Olsen, E. T., Fishbein, E., Lee, S. Y., Manning, E., Maddy, E., and McMillan, W. W.: AIRS/AMSU/HSB Version 5 Level 2 Product Levels, Layers and Trapezoids, Retrieval Channel Sets, Jet Propulsion Laboratory, California Institute of Technology, Pasadena, CA, 2007.
Omar, A. H., Winker, D. M., Kittaka, C., Vaughan, M. A., Liu, Z. Y., Hu, Y. X., Trepte, C. R., Rogers, R. R., Ferrare, R. A., Lee, K. P., Kuehn, R. E., and Hostetler, C. A.: The CALIPSO automated aerosol classification and lidar ratio selection algorithm, J. Atmos. Ocean. Technol., 26, 1994–2014, doi:10.1175/2009JTECHA1231.1, 2009.
Pouliot, G., Pierce, T., Benjey, W., O'Neill, S. M., Ferguson, S. A.: Wildfire emission modeling: integrating BlueSky and SMOKE, in: Presentation at the 14th International Emission Inventory Conference, Transforming Emission Inventories Meeting Future Challenges Today, 11 April–14 April 2005, Las Vegas, NV, Session 12, available at: http://www.epa.gov/ttn/chief/conference/ei14/session12/pouliot.pdf, 2005.
Raffuse, S. M., Pryden, D. A., Sullivan, D. C., Larkin, N. K., Strand, T., and Solomon., R.: SMARTFIRE algorithm description, report, Sonoma Technol. Inc., Petaluma, Calif., 2009.
Raffuse, S. M., Craig, K. J., Larkin, N. K., Strand, T. T., Sullivan, D. C., Wheeler, N. J. M., and Solomon, R.: An evaluation of modeled plume injection height with satellite-derived observed plume height, Atmosphere, 3, 103–123, doi:10.3390/atmos3010103, 2012.
Remer, L. A., Kaufman, Y. J., Tanre, D., Mattoo, S., Chu, D. A., Martins, J. V., Li, R. R., Ichoku, C., Levy, R. C., Kleidman, R. G., Eck, T. F., Vermote, E., and Holben, B. N.: The modis aerosol algorithm, products, and validation, J. Atmos. Sci., 62, 947–973, doi:10.1175/JAS3385.1, 2005.
Riccardi, C. L., Prichard, S. J., Sandberg, D. V., and Ottmar, R. D.: Quantifying physical characteristics of wildland fuels using the fuel characteristic classification system, Can. J. Forest Res., 37, 2413–2420, 2007.
Roy, B., Mathur, R., Gilliland, A. B., and Howard, S. C.: A comparison of CMAQ-based aerosol properties with IMPROVE, MODIS, and AERONET data, J. Geophys. Res., 112, D14301, doi:10.1029/2006JD008085, 2007.

ACPD
14, 11103–11152, 2014

Seinfeld, J. H. and Pandis, S. N.: Atmospheric Chemistry and Physics: From Air Pollution to Climate Change, J. Wiley, New York, 1998.
Simon, H. and Bhave, P. V.: Simulating the degree of oxidation in atmospheric organic particles, Environ. Sci. Technol., 46, 331–339, 2012.
Skamarock, W. C., Klemp, J. B., Dudhia, J., Gill, D. O., Barker, D. M., Wang, W., and Powers, J. G.: A Description of the Advanced Research WRF Version 2, National Center for Atmosphreric Research, Boulder, Colorado, 2005.
Strand, T., Larkin, N. K., Rorig, M., Krull, C., Moore, M.: $PM_{2.5}$ measurements in wildfire smoke plumes from fire seasons 2005–2008 in the Northwestern United States, J. Aerosol Sci., 42, 3, 143–155, 2011.
Strand, T. M., Larkin, N., Solomon, R., Rorig, N., Craig, K. J., Raffuse, S., Sullivan, D., Wheeler, N., and Pryden, D.: Analyses of BlueSky Gateway $PM_{2.5}$ predictions during the 2007 southern and 2008 northern California fires, J. Geophys. Res., 117, D17301, doi:10.1029/2012JD017627, 2012.
Vaughan, M., Winker, D., and Powell, K.: CALIOP Algorithm Theoretical Basis Document, part 2, Feature detection and layer properties algorithms, PC-SCI-202.01, NASA Langley Res. Cent., Hampton, Va, available at: http://www-calipso.larc.nasa.gov/resources/pdfs/PC-SCI-202_Part2_rev1x01.pdf (last access: 27 April 2014), 2005.
Weiss-Penzias, P., Jaffe, D. A., Swartzendruber, P., Dennison, J. B., Chand, D., Hafner, W., and Prestbo, E.: Observations of Asian air pollution in the free troposphere at Mt. Bachelor Observatory in the spring of 2004, J. Geophys. Res., 110, D10304, doi:10.1029/2005JD006522, 2006.
Wespes, C., Emmons, L., Edwards, D. P., Hannigan, J., Hurtmans, D., Saunois, M., Coheur, P.-F., Clerbaux, C., Coffey, M. T., Batchelor, R. L., Lindenmaier, R., Strong, K., Weinheimer, A. J., Nowak, J. B., Ryerson, T. B., Crounse, J. D., and Wennberg, P. O.: Analysis of ozone and nitric acid in spring and summer Arctic pollution using aircraft, ground-based, satellite observations and MOZART-4 model: source attribution and partitioning, Atmos. Chem. Phys., 12, 237–259, doi:10.5194/acp-12-237-2012, 2012.
Wiedinmyer, C., Akagi, S. K., Yokelson, R. J., Emmons, L. K., Al-Saadi, J. A., Orlando, J. J., and Soja, A. J.: The Fire INventory from NCAR (FINN): a high resolution global model to estimate the emissions from open burning, Geosci. Model Dev., 4, 625–641, doi:10.5194/gmd-4-625-2011, 2011.

Wigder, N. L., Jaffe, D. A., Saketa, F. A.: Ozone and Particulate Matter Enhancements from Regional Wildfires Observed at Mount Bachelor during 2004–2011, Atmos. Environ., 75, 24–31, doi:10.1016/j.atmosenv.2013.04.026, 2013.

Winker, D. M., Vaughan, M. A., Omar, A., Hu, Y., Powell, K. A., Liu, Z., Hunt, W. H., and Young, S. A.: Overview of the CALIPSO mission and CALIOP data processing algorithms, J. Atmos. Ocean. Technol., 26, 2310–2323, doi:10.1175/2009JTECHA1281.1, 2009.

Wong, D. C., Pleim, J., Mathur, R., Binkowski, F., Otte, T., Gilliam, R., Pouliot, G., Xiu, A., Young, J. O., and Kang, D.: WRF-CMAQ two-way coupled system with aerosol feedback: software development and preliminary results, Geosci. Model Dev., 5, 299–312, doi:10.5194/gmd-5-299-2012, 2012.

Table 1a. Total annual fires and acres burned by state.

State	2007 Total Fires	Total Acres	2008 Total Fires	Total Acres
California	10 034	1 160 297	6670	1 456 758
Idaho	2064	2 226 769	1546	225 832
Montana	2342	859 977	1749	211 593
Nevada	924	905 237	491	90 868
Oregon	3424	758 740	2561	252 671
Utah	1527	664 754	1139	66 170
Washington	2578	249 708	1418	154 368
USA Grand Totals	110 237	12 899 948	88 059	7 433 094

NIFC ource: National Interagency Fire Center
(http://www.nifc.gov/fireInfo/fireInfo_statistics.html).

ACPD
14, 11103–11152, 2014

Air quality simulations of wildfires in the Pacific Northwest

F. L. Herron-Thorpe et al.

Table 1b. Details of the largest fires reported during the analysis periods (3 July–22 August 2007 and 22 June–27 August 2008). Locations are indicated by the National Forest (NF) affected if applicable. Fires not completely contained before the end of analysis period are marked ([a]). The area burned reported here is only an approximate of the area burned during the analysis period thus fires not completely contained before the end of the analysis period likely burned additional area not included below.

Fire/Complex Name	State(s)	Location	Ignition Date(s)	Days to Contain	Acres Burned
Egley Complex	OR	north of Riley, OR	6 Jul 2007	18	140 000
East Zone Complex	ID	Payette NF and Boise NF	6 Jul 2007	[a]	200 000
Rattlesnake Complex	ID	Nez Perce NF	6 Jul 2007	[a]	90 000
Murphy Complex	ID, NV	southwest Idaho and northeast Nevada	16 Jul 2007	19	652 000
Cascade Complex	ID	Boise NF, Payette NF, and Salmon-Challis NF	16 Jul 2007	[a]	211 000
Hepworth Complex	NV	surrounding Wells, NV	16 Jul 2007	9	58 000
Shower Bath Complex	ID	Salmon-Challis NF	29 Jul–2 Aug 2007	[a]	100 000
Chippy Creek Fire	ID, MT	Kootenai NF	29 Jul–2 Aug 2007	[a]	96 000
Sawmill Complex	MT	Lolo NF and Beaverhead-Deerlodge NF	29 Jul–2 Aug 2007	[a]	55 000
Fool Creek Fire	MT	Lewis-Clark NF	29 Jul–2 Aug 2007	[a]	60 000
Jocko Lakes Fire	MT	surrounding Seeley Lake, MT	29 Jul–2 Aug 2007	[a]	35 000
Brush Creek Fire	MT	Flathead NF	29 Jul–2 Aug 2007	[a]	30 000
Iron-Alps Complex	CA	Shasta-Trinity NF	21 Jun 2008	[a]	100 000
Lime Complex	CA	Shasta-Trinity NF	21 Jun 2008	[a]	65 000
Klamath Theater Complex	CA	Klamath NF	21 Jun 2008	[a]	50 000
Shu Lightning Complex	CA	Shasta-Trinity NF	21 Jun	[a]	20 000

ACPD
14, 11103–11152, 2014

Air quality simulations of wildfires in the Pacific Northwest

F. L. Herron-Thorpe et al.

Table 2. Definitions of Model Performance Statistics (Chen et al., 2008).

Measured Concentration	O_i
Predicted Concentration	M_i
Number of Paired Data Points	N
Predicted Mean ($\overline{M}$)	$\frac{1}{N}\sum_{i=1}^{N} M_i$
Measured Mean ($\overline{O}$)	$\frac{1}{N}\sum_{i=1}^{N} O_i$
Mean Bias (MB)	$\frac{1}{N}\sum_{i=1}^{N}(M_i - O_i)$
Mean Error (ME)	$\frac{1}{N}\sum_{i=1}^{N}\lvert M_i - O_i\rvert$
Normalized Mean Bias (NMB), %	$\frac{1}{N}\sum_{i=1}^{N}(M_i - O_i)/O_i$
Normalized Mean Error (NME), %	$\frac{1}{N}\sum_{i=1}^{N}\lvert M_i - O_i\rvert/O_i$
Fractional Bias (FB), %	$\frac{1}{N}\sum_{i=1}^{N}\frac{(M_i - O_i)}{0.5(M_i + O_i)}$
Fractional Error (FE), %	$\frac{1}{N}\sum_{i=1}^{N}\frac{\lvert M_i - O_i\rvert}{0.5(M_i + O_i)}$
Correlation Coefficient (r)	$\frac{\sum_{i=1}^{N}(M_i - \overline{M})(O_i - \overline{O})}{\left[\sum_{i=1}^{N}(M_i - \overline{M})^2 \cdot \sum_{i=1}^{N}(O_i - \overline{O})^2\right]^{1/2}}$

ACPD
14, 11103–11152, 2014

Table 3. Summary of model performance statistics for 3 July to 23 August 2007.

Species	A24 h $PM_{2.5}$		MDA8 h Ozone		AOD		Column CO		Trop. Col. NO_2	
Obs. Data Source	EPA AQS		EPA AQS		Aqua/MODIS		AIRS		OMI	
Plume Rise Method	FEPS	SMOKE	FEPS	SMOKE	FEPS	SMOKE	FEPS	SMOKE	FEPS	SMOKE
Paired Points	3267	3267	450	450	3603	3603	4275	4275	5821	5821
Correlation (r)	0.48	0.60	0.72	0.70	0.37	0.29	0.60	0.52	0.44	0.44
Measured Mean	7.12	7.12	45.8	45.8	0.17	0.17	1.83E+18	1.83E+18	1.40E+15	1.40E+15
Mean Bias	0.44	−0.72	−4.60	−3.54	−0.10	−0.10	−0.22E+18	−0.17E+18	−0.46E+15	−0.47E+15
Mean Error	5.56	4.13	8.93	8.97	0.12	0.12	0.24E+18	0.23E+18	0.92E+15	0.92E+15
Normalized Mean Bias	−0.02	−0.09	−0.07	−0.04	−0.23	−0.15	−0.12	−0.09	1.10	1.04
Normalized Mean Error	0.63	0.54	0.20	0.21	0.77	0.85	0.13	0.12	1.89	1.82
Fractional Bias (%)	−34.0	−32.9	−10.3	−8.10	−65.9	−61.3	−13.0	−10.3	−37.7	−39.2
Fractional Error (%)	59.6	56.5	21.5	21.2	91.0	89.5	13.9	13.2	75.4	76.1

Note that negative values in the observational data are masked.

ACPD
14, 11103–11152, 2014

Air quality simulations of wildfires in the Pacific Northwest

F. L. Herron-Thorpe et al.

Table 4. Summary of matched-threshold model performance statistics for 3 Jul to 23 Aug 2007. Note that satellite results use rural sites only.

Species	A24 h $PM_{2.5}$		AOD		Column CO		Trop. Col. NO_2	
Obs. Data Source	EPA AQS		Aqua/MODIS		AIRS		OMI	
Plume Rise Method	FEPS	SMOKE	FEPS	SMOKE	FEPS	SMOKE	FEPS	SMOKE
Threshold	10 $\mu g\, m^{-3}$		0.3		1.9E+18 VCD		1.0E+15 VCD	
Paired Points	555	555	150	150	356	356	599	599
Correlation (r)	0.41	0.48	0.03	0.02	0.28	0.38	0.19	0.19
Measured Mean	16.8	16.8	0.49	0.49	2.05E+18	2.05E+18	1.7E+15	1.7E+15
Mean Bias	5.9	−0.1	−0.34	−0.25	−0.32E+18	−0.15E+18	−1.1E+15	−1.1E+15
Mean Error	19.1	12.1	0.39	0.41	0.36E+18	0.39E+18	1.2E+15	1.2E+15
Normalized Mean Bias	0.24	−0.03	−0.66	−0.47	−0.15	−0.08	−0.59	−0.60
Normalized Mean Error	1.04	0.70	0.77	0.84	0.17	0.19	0.68	0.68
Fractional Bias (%)	−38.3	−35.9	−117.3	−101.1	−17.6	−10.1	−96.5	−98.1
Fractional Error (%)	79.6	70.1	122.9	114.9	19.2	19.1	100.8	101.8

Note "Matched Threshold" refers to both model and observation values being removed from the analysis if either is below the threshold.

ACPD
14, 11103–11152, 2014

Air quality simulations of wildfires in the Pacific Northwest

F. L. Herron-Thorpe et al.

Table 5. Summary of model performance statistics for 22 June to 27 August 2008.

Species	A24 h $PM_{2.5}$		MDA8 h Ozone		AOD		Column CO		Trop. Col. NO_2	
Obs. Data Source	EPA AQS		EPA AQS		Aqua/MODIS		AIRS		OMI	
Plume Rise Method	FEPS	SMOKE	FEPS	SMOKE	FEPS	SMOKE	FEPS	SMOKE	FEPS	SMOKE
Paired Points	5329	5329	1135	1135	5125	5125	4577	4577	7760	7760
Correlation (r)	0.04	0.37	0.77	0.75	0.31	0.29	0.68	0.58	0.46	0.47
Measured Mean	6.82	6.82	42.3	42.3	0.19	0.19	1.89E+18	1.89E+18	1.28E+15	1.28E+15
Mean Bias	0.27	−0.68	−0.74	0.19	−0.11	−0.10	−0.14E+18	−0.09E+18	−0.30E+15	−0.32E+15
Mean Error	5.41	4.05	7.73	7.97	0.14	0.14	0.18E+18	0.19E+18	0.81E+15	0.80E+15
Normalized Mean Bias	0.34	0.05	0.03	0.05	−0.09	0.18	−0.07	−0.04	1.10	1.06
Normalized Mean Error	0.98	0.66	0.21	0.21	0.85	1.08	0.09	0.09	1.76	1.73
Fractional Bias (%)	−31.2	−26.8	−0.89	0.91	−57.8	−52.5	−7.30	−4.9	−26.1	−27.9
Fractional Error (%)	61.8	60.1	20.0	20.0	87.9	83.7	9.40	9.60	70.0	70.2

Note that negative values in the observational data are masked.

ACPD
14, 11103–11152, 2014

Table 6. Summary of matched-threshold model performance statistics for 22 June to 27 August 2008. Note that satellite results use rural sites only.

Species	A24 h $PM_{2.5}$		AOD		Column CO		Trop. Col. NO_2	
Obs. Data Source	EPA AQS		Aqua/MODIS		AIRS		OMI	
Plume Rise Method	FEPS	SMOKE	FEPS	SMOKE	FEPS	SMOKE	FEPS	SMOKE
Threshold	$10\,\mu g\,m^{-3}$		0.3		1.9E+18 VCD		1.0E+15 VCD	
Paired Points	872	872	260	260	521	521	755	755
Correlation (r)	0.39	0.38	0.14	0.28	0.29	0.21	0.29	0.30
Measured Mean	15.9	15.9	0.51	0.51	2.14E+18	2.14E+18	1.6E+15	1.6E+15
Mean Bias	−6.5	−5.6	−0.38	−0.30	−0.25E+18	−0.19E+18	−0.9E+15	−0.9E+15
Mean Error	9.0	8.4	0.40	0.40	0.29E+18	0.28E+18	1.1E+15	1.1E+15
Normalized Mean Bias	−0.35	−0.33	−0.73	−0.59	−0.11	−0.08	−0.54	−0.57
Normalized Mean Error	0.56	0.53	0.77	0.75	0.12	0.12	0.66	0.66
Fractional Bias (%)	−66.4	−56.7	−125.3	−104.6	−12.0	−9.08	−90.4	−92.6
Fractional Error (%)	77.1	70.5	128.3	113.4	13.6	13.1	95.3	96.5

Note "Matched Threshold" refers to both model and observation values being removed from the analysis if either is below the threshold.

ACPD
14, 11103–11152, 2014

Air quality simulations of wildfires in the Pacific Northwest

F. L. Herron-Thorpe et al.

ACPD
14, 11103–11152, 2014

Air quality simulations of wildfires in the Pacific Northwest

F. L. Herron-Thorpe et al.

Table 7. Summary of the plume top height comparisons: CALIOP vs. AIRPACT-3 for both a.g.l. and a.m.s.l.. Please note that some plumes contribute multiple paired points.

Year Plume Rise Method Vertical Reference	2007 FEPS a.g.l.	2007 FEPS a.m.s.l.	2007 SMOKE a.g.l.	2007 SMOKE a.m.s.l.	2008 FEPS a.g.l.	2008 FEPS a.m.s.l.	2008 SMOKE a.g.l.	2008 SMOKE a.m.s.l.
Paired Points	219	219	218	218	275	275	281	281
Correlation (r)	−0.02	0.20	0.15	0.38	0.62	0.80	0.54	0.77
Measured Mean (km)	5.19	8.17	5.08	8.04	3.48	5.59	3.47	5.62
Mean Bias (km)	−1.41	−3.08	−1.47	−3.13	−1.02	−2.27	−0.93	−2.20
Mean Error (km)	2.07	3.27	1.93	3.20	1.28	2.31	1.24	2.24
Normalized Mean Bias	−0.03	−0.34	−0.10	−0.35	−0.16	−0.39	−0.10	−0.35
Normalized Mean Error	0.52	0.38	0.45	0.38	0.43	0.40	0.42	0.36
Fractional Bias (%)	−28.4	−45.6	−27.6	−45.7	−32.3	−51.5	−26.4	−46.0
Fractional Error (%)	45.8	48.5	44.8	48.2	44.6	52.7	42.3	47.6

Table 8. $PM_{2.5}$ National Ambient Air Quality Standards summary for both 2007 and 2008 fire periods analyzed per site per day.

Summary of 24 h NAAQS Threshold (35 µg m^{-3})						
FEPS Plume Rise Scenario						
Year	Monitors	Days	Matched Exceedances	Predictions Unmatched	Observations Unmatched	No Exceedances
2007	67	51	12	77	10	3168
2008	82	67	5	74	19	5231
		Totals:	17	151	29	8399
		Percent:	0.2 %	1.8 %	0.3 %	97.7 %
SMOKE Plume Rise Scenario						
Year	Monitors	Days	Matched Exceedances	Predictions Unmatched	Observations Unmatched	No Exceedances
2007	67	51	12	56	10	3189
2008	82	67	4	54	20	5251
		Totals:	16	110	30	8440
		Percent:	0.2 %	1.3 %	0.3 %	98.2 %
Summary of Annual NAAQS Threshold (12 µg m^{-3})						
FEPS Plume Rise Scenario						
Year	Monitors	Days	Matched Exceedances	Predictions Unmatched	Observations Unmatched	No Exceedances
2007	67	51	157	206	242	5929
2008	82	67	146	393	454	9665
		Totals:	303	599	696	15 594
		Percent:	1.8 %	3.5 %	4.0 %	90.7 %
SMOKE Plume Rise Scenario						
Year	Monitors	Days	Matched Exceedances	Predictions Unmatched	Observations Unmatched	No Exceedances
2007	67	51	169	181	230	5954
2008	82	67	186	427	414	9631
		Totals:	355	608	644	15 585
		Percent:	2.1 %	3.5 %	3.7 %	90.7 %

ACPD
14, 11103–11152, 2014

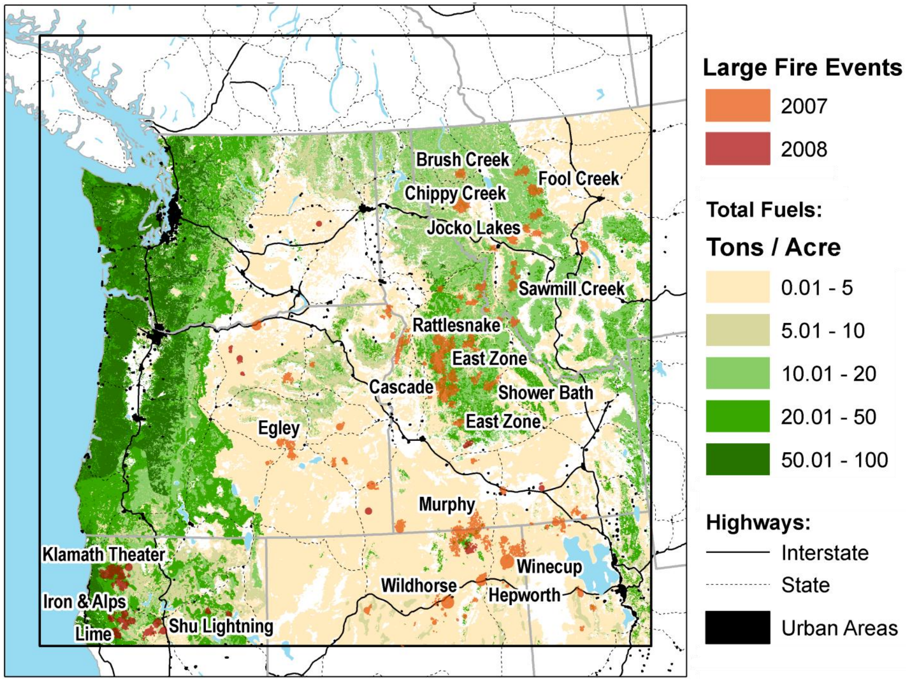

Fig. 1. Fire events with individual burn areas greater than 5000 acres during the analysis periods of 2007 (orange) and 2008 (red). Total fuel loading derived from the FCCS v1 is also shown for the AIRPACT-3 domain.

ACPD
14, 11103–11152, 2014

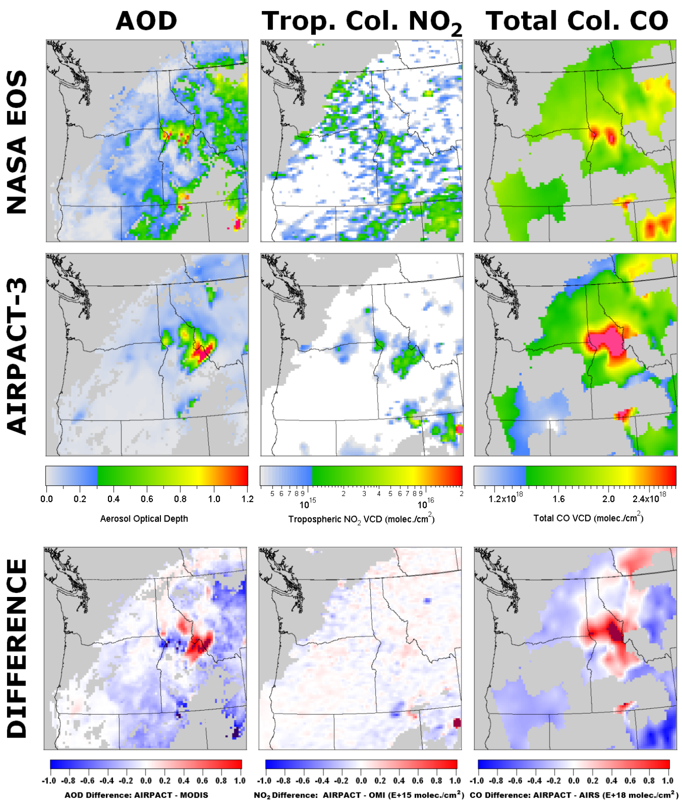

Fig. 2. AOD (left column), tropospheric NO_2 columns (middle column), and total carbon monoxide columns (right column) for 22 July 2007 (∼ 2 p.m. LST) with NASA EOS retrieval (top row), AIRPACT-3 with SMOKE plume rise (middle row), and differences (bottom row). Grey color indicates no or low-quality data from the satellite retrieval exclusion from analysis. Values greater than the color scale maximum are shown as pink in the AIRPACT-3 and NASA EOS maps. Values outside the range of the difference color scales are shown as saturated blue/red.

ACPD
14, 11103–11152, 2014

Air quality simulations of wildfires in the Pacific Northwest

F. L. Herron-Thorpe et al.

Title Page
Abstract | Introduction
Conclusions | References
Tables | Figures
◀◀ | ▶▶
◀ | ▶
Back | Close
Full Screen / Esc
Printer-friendly Version
Interactive Discussion

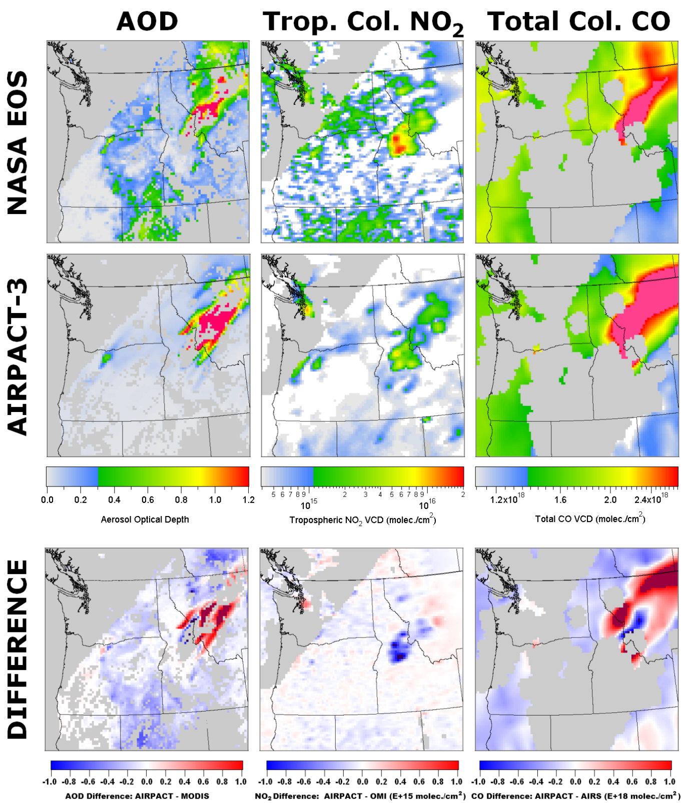

Fig. 3. AOD (left column), tropospheric NO_2 columns (middle column), and total carbon monoxide columns (right column) for 12 August 2007 (~ 2 p.m. LST) with NASA EOS retrieval (top row), AIRPACT-3 with SMOKE plume rise (middle row), and differences (bottom row). Grey color indicates no or low-quality data from the satellite retrieval exclusion from analysis. Values greater than the color scale maximum are shown as pink in the AIRPACT-3 and NASA EOS maps. Values outside the range of the difference color scales are shown as saturated blue/red.

ACPD
14, 11103–11152, 2014

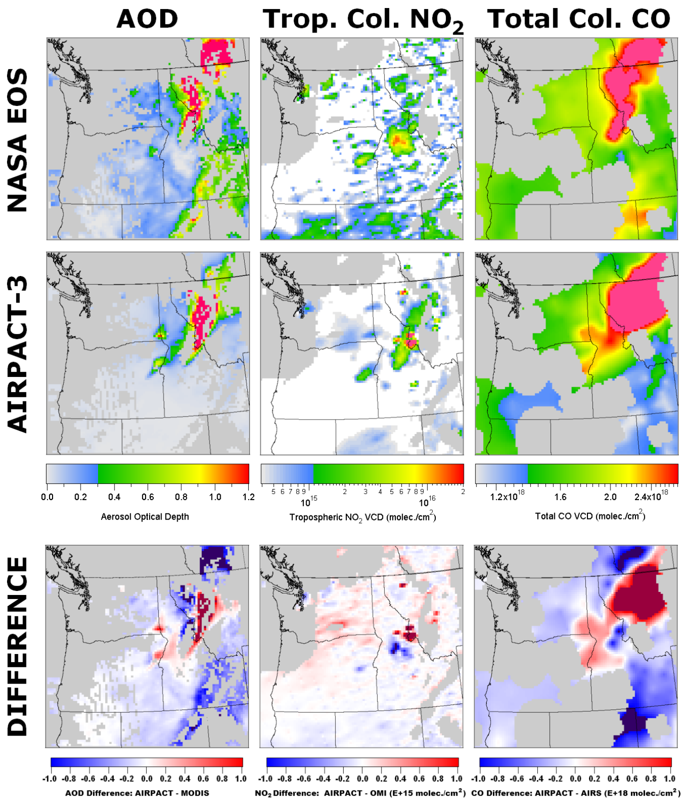

Fig. 4. AOD (left column), tropospheric NO_2 columns (middle column), and total carbon monoxide columns (right column) for 18 August 2007 (~ 2 p.m. LST) with NASA EOS retrieval (top row), AIRPACT-3 with SMOKE plume rise (middle row), and differences (bottom row). Grey color indicates no or low-quality data from the satellite retrieval exclusion from analysis. Values greater than the color scale maximum are shown as pink in the AIRPACT-3 and NASA EOS maps. Values outside the range of the difference color scales are shown as saturated blue/red.

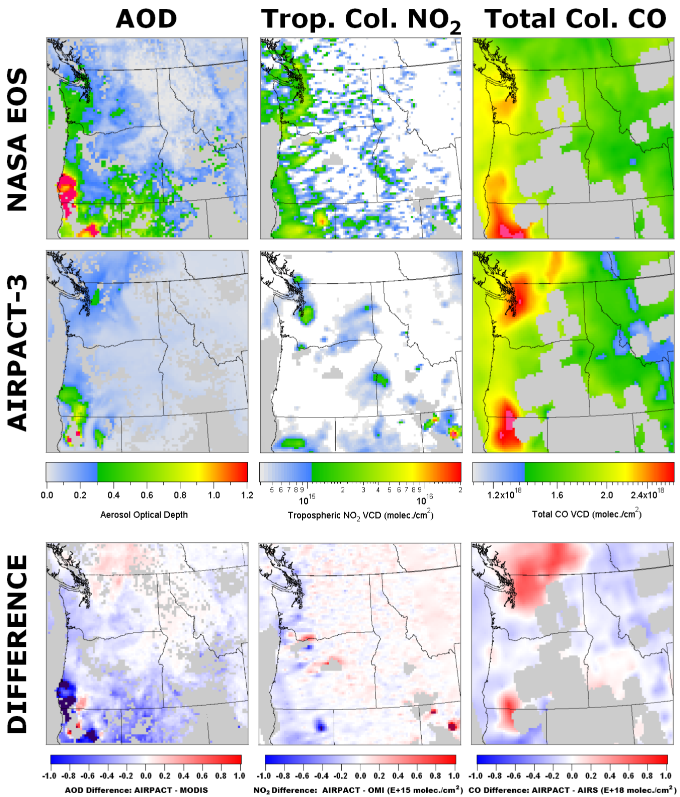

Fig. 5. AOD (left column), tropospheric NO_2 columns (middle column), and total carbon monoxide columns (right column) for 29 June 2008 (~ 2 p.m. LST) with NASA EOS retrieval (top row), AIRPACT-3 with SMOKE plume rise (middle row), and differences (bottom row). Grey color indicates no or low-quality data from the satellite retrieval exclusion from analysis. Values greater than the color scale maximum are shown as pink in the AIRPACT-3 and NASA EOS maps. Values outside the range of the difference color scales are shown as saturated blue/red.

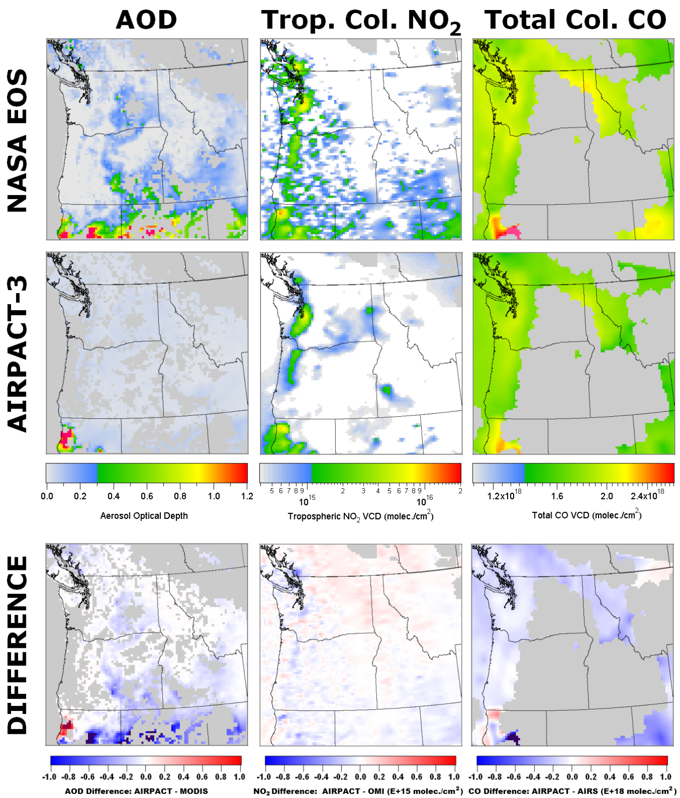

Fig. 6. AOD (left column), tropospheric NO_2 columns (middle column), and total carbon monoxide columns (right column) for 11 July 2008 (~ 2 p.m. LST) with NASA EOS retrieval (top row), AIRPACT-3 with SMOKE plume rise (middle row), and differences (bottom row). Grey color indicates no or low-quality data from the satellite retrieval excluded from analysis. Values greater than the color scale maximum are shown as pink in the AIRPACT-3 and NASA EOS maps. Values outside the range of the difference color scales are shown as saturated blue/red.

ACPD
14, 11103–11152, 2014

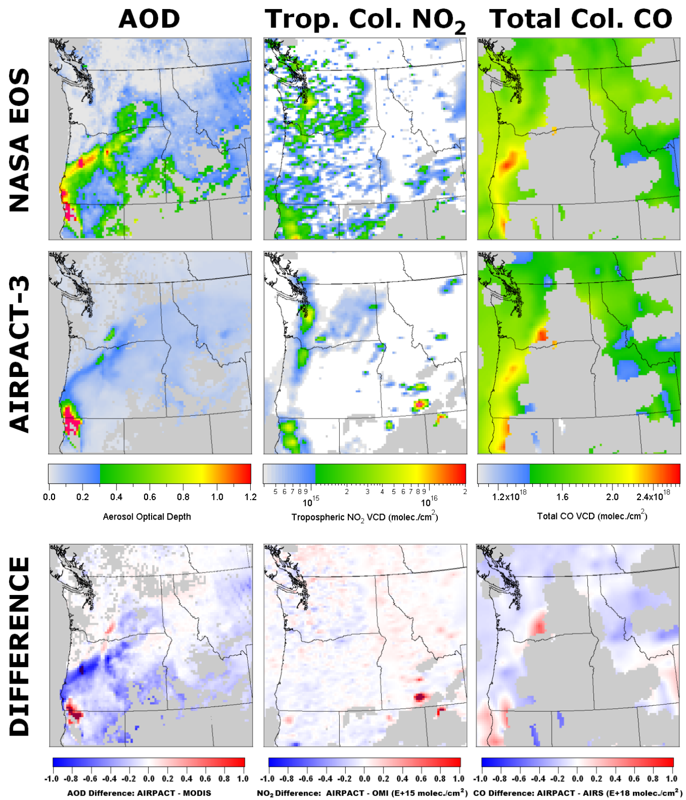

Fig. 7. AOD (left column), tropospheric NO_2 columns (middle column), and total carbon monoxide columns (right column) for 20 July 2008 (~ 2 p.m. LST) with NASA EOS retrieval (top row), AIRPACT-3 with SMOKE plume rise (middle row), and differences (bottom row). Grey color indicates no or low-quality data from the satellite retrieval exclusion from analysis. Values greater than the color scale maximum are shown as pink in the AIRPACT-3 and NASA EOS maps. Values outside the range of the difference color scales are shown as saturated blue/red.

ACPD
14, 11103–11152, 2014

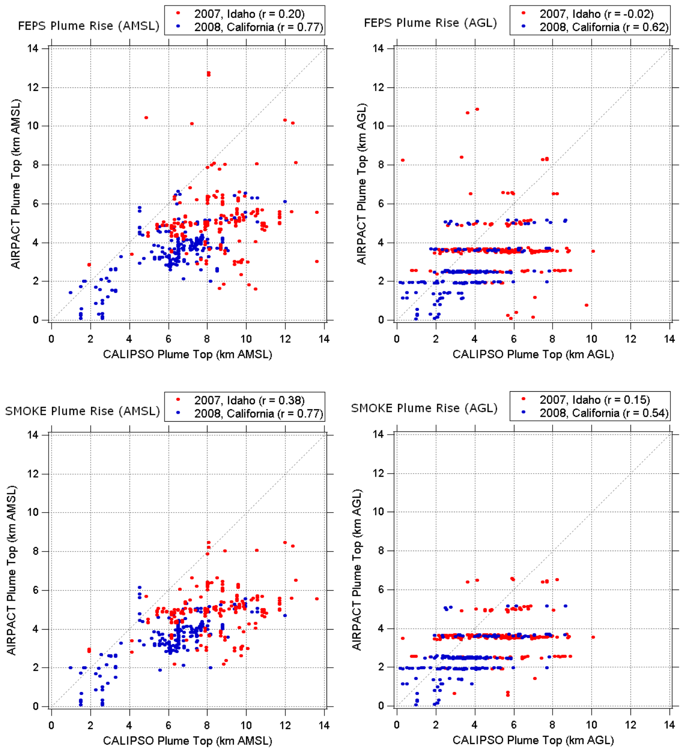

Fig. 8. AIRPACT-3 vs. CALIOP plume top heights for 2007 (red) and 2008 (blue) when CALIPSO passed over the Idaho and California wildfires, respectively (~ 2 p.m. LST). Plume top heights a.s.l. (left) and a.g.l. (right) are shown for both the FEPS plume rise (top) and SMOKE plume rise (bottom) scenarios. Note that plume top heights are only shown for locations where both CALIOP and AIRPACT-3 showed an aerosol plume.

ACPD
14, 11103–11152, 2014

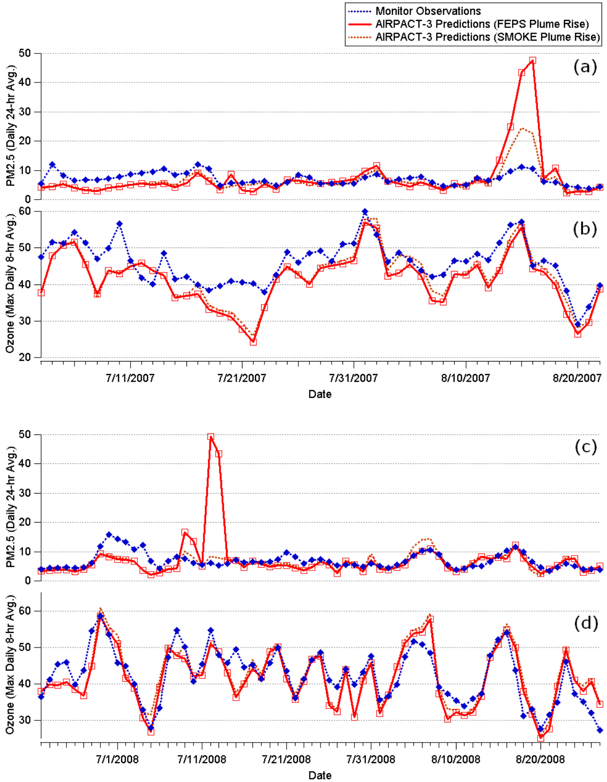

Fig. 9. (top) Daily 24 h average $PM_{2.5}$ averaged across 67 sites **(a)** and max daily 8 h average ozone averaged across 10 sites **(b)** from 3 July to 22 August 2007; (bottom) daily 24 h average $PM_{2.5}$ averaged across 82 sites **(c)** and max daily 8 h average ozone averaged across 18 sites **(d)** from 22 June to 27 August 2008. Model simulations are shown in red with squares (FEPS plume rise) and orange dotted (SMOKE plume rise) while observations are shown in dotted blue with diamonds.

ACPD
14, 11103–11152, 2014

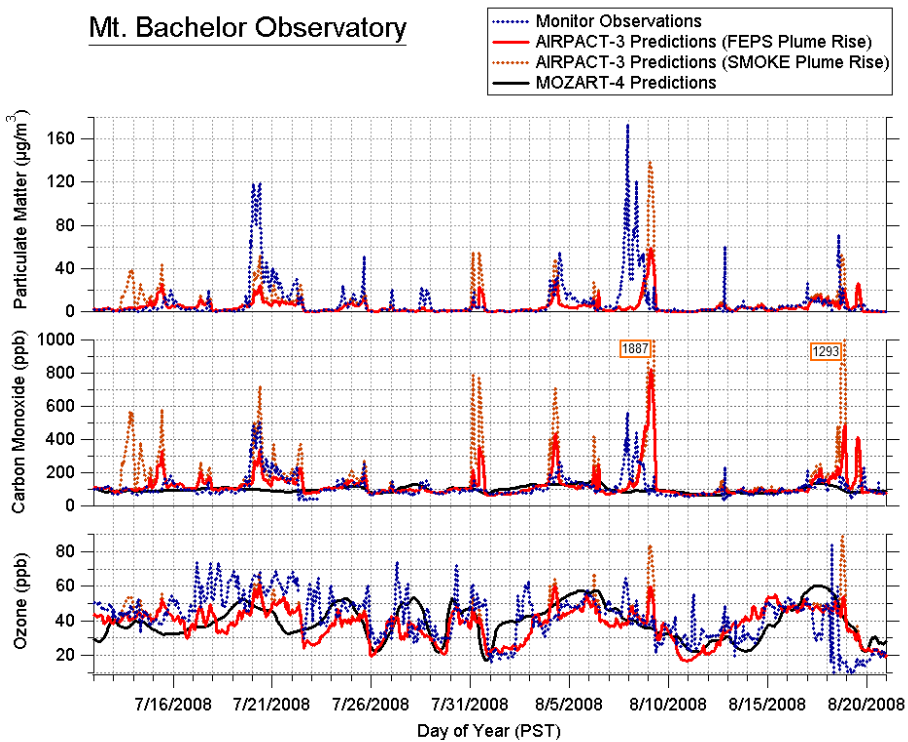

Fig. 10. Particulate matter (top), carbon monoxide (middle), and ozone (bottom) at Mt. Bachelor Observatory for 12 July to 21 August 2008. AIRPACT-3 model simulations are shown in red (FEPS plume rise) and orange (SMOKE plume rise), MOZART-4 model simulations are shown in black, and observations are shown in dotted blue. Note that aerosols for AIRPACT-3 are reported as $PM_{2.5}$ and observed aerosols are sub-micron aerosols converted from scattering observations using the method described in Wigder et al. (2013).

ACPD
14, 11103–11152, 2014